Thesis for the Degree of Doctor of Philosophy

All-optical nonlinearity mitigation in fiber-optic communications

Henrik Eliasson

CHALMERS

Photonics Laboratory
Department of Microtechnology and Nanoscience (MC2)
Chalmers University of Technology
Göteborg, Sweden, 2018

All-optical nonlinearity mitigation in fiber-optic communications

Henrik Eliasson

Göteborg, April 2018

ISBN 978-91-7597-728-7

Doktorsavhandlingar vid Chalmers Tekniska Högskola
Ny serie 4409
ISSN 0346-718X

Technical Report MC2-385
ISSN 1652-0769

Chalmers University of Technology
Microtechnology and Nanoscience (MC2)
Photonics Laboratory
SE-412 96 Göteborg, Sweden
Phone: +46 (0) 31 772 1000

Front cover illustration: (left) A QPSK constellation with three symbol transitions marked. (right) The same three transitions of the phase-conjugated copy.

Printed by Chalmers reproservice, Chalmers University of Technology
Göteborg, Sweden, April, 2018

All-optical nonlinearity mitigation in fiber-optic communications

Henrik Eliasson

Chalmers University of Technology
Department of Microtechnology and Nanoscience (MC2)
Photonics Laboratory, SE-412 96 Göteborg, Sweden

Abstract

The two main factors limiting the data throughput in modern fiber-optic communication links are the noise added by amplifiers and the nonlinear response of the optical fiber due to the Kerr effect. Today there are communication systems operating remarkably close to the limits set by these two factors. In order to increase the data throughput in a single fiber one can attempt reducing the noise added by the amplifiers or mitigate the nonlinear distortion which is dominated by deterministic effects.

The work presented in this thesis is focused on reducing the negative impact of the Kerr nonlinearity through the use of all-optical signal processing by transmission of a phase-conjugated copy alongside the signal. A concept where the phase-conjugated data is repeated in time domain is investigated and it was found that it performs comparably to the conventional phase-conjugated twin waves concept. The rest of the thesis is dedicated to studying various aspects of the two-mode copier-phase-sensitive amplifier (PSA) scheme. These studies focus both on improving the understanding and on optimizing the performance of the nonlinearity mitigation in copier-PSA links. We study the optimization of the dispersion map on a single- and two-span basis and it is shown in simulations that significant improvements can be achieved by optimization over two spans. In a numerical study it was found that there is potential for improving the efficiency of the nonlinearity mitigation by addition of distributed Raman amplification (DRA) in a copier-PSA link. Long-haul transmission using the copier-PSA scheme is demonstrated experimentally both with and without DRA. Without DRA at 10 Gbaud, it is shown that it is possible to improve the transmission reach by up to a factor of 5.6 with the addition of PSAs. With DRA at 28 Gbaud, the improvement in transmission reach is smaller but we observe an increase in the optimum launch power when enabling the PSAs indicating improved nonlinearity mitigation.

Keywords: fiber-optic communication, nonlinear optics, phase-sensitive amplifiers, optical phase conjugation

List of papers

This thesis is based on the following appended papers:

[A] **H. Eliasson**, P. Johannisson, M. Karlsson and P. A. Andrekson, "Mitigation of nonlinearities using conjugate data repetition," *Optics Express*, vol. 23, no. 3, pp. 2392-2402, 2015.

[B] **H. Eliasson**, S. L. I. Olsson, M. Karlsson and P. A. Andrekson, "Comparison between coherent superposition in DSP and PSA for mitigation of nonlinearities in a single-span link," Proceedings European Conference on Optical Communication (ECOC), Cannes, France, 2015, paper Mo.2.5.2.

[C] **H. Eliasson**, S. L. I. Olsson, M. Karlsson and P. A. Andrekson, "Mitigation of nonlinear distortion in hybrid Raman/phase-sensitive amplifier links," *Optics Express*, vol. 24, no. 2, pp. 888-900, 2016.

[D] E. Astra, S. L. I. Olsson, **H. Eliasson** and P. A. Andrekson, "Dispersion management for nonlinearity mitigation in two-span 28 GBaud QPSK phase-sensitive amplifier links," *Optics Express*, vol. 25, no. 12, pp. 13163-13173, 2017.

[E] S. L. I. Olsson, **H. Eliasson**, E. Astra, M. Karlsson and P. A. Andrekson, "Long-haul optical transmission links using low-noise phase-sensitive amplifiers," Manuscript under review.

[F] **H. Eliasson**, K. Vijayan, B. Foo, S. L. I. Olsson, E. Astra, M. Karlsson and P. A. Andrekson, "Phase-sensitive amplifier links with distributed Raman amplification," Manuscript to be submitted.

Related publications and conference contributions by the author not included in the thesis:

[G] **H. Eliasson**, P. Johannisson, H. Sunnerud, M. Westlund, M. Karlsson and P. Andrekson, "Transmitter mask testing for 28 GBaud PM-QPSK," Proceedings European Conference on Optical Communication (ECOC), London, UK, 2013, paper Tu.3.C.2.

[H] C. Lundström, **H. Eliasson**, I. Fatadin, P. Johannisson, P. Andrekson and M. Karlsson, "Mask testing of 28 GBaud 16-QAM transmitters using time-resolved error vector magnitude," Proceedings Signal Processing in Photonic Communications (SPPCom), Boston, USA, 2015, paper SpS4D.3.

[I] E. Astra, Samuel. L. I. Olsson, **H. Eliasson**, T. Laadung, P. A. Andrekson "Dispersion map optimization for nonlinearity mitigation in two-span phase-sensitive amplifier links," Proceedings European Conference on Optical Communication (ECOC), Düsseldorf, Germany, 2016, paper Th.1.A.3

[J] **H. Eliasson**, S. L. I. Olsson, M. Karlsson and P. A. Andrekson "Experimental investigation of nonlinearity mitigation properties of a hybrid distributed Raman/phase-sensitive amplifier link," Proceedings Optical Fiber Communication Conference (OFC), Los Angeles, USA, 2017, paper Th3J.4.

[K] C. Fougstedt, M. Mazur, L. Svensson, **H. Eliasson**, M. Karlsson and P. Larsson-Edefors "Time-domain digital back propagation: algorithm and finite-precision implementation aspects," Proceedings Optical Fiber Communication Conference (OFC), Los Angeles, USA, 2017, paper W1G.4.

[L] E. Astra, **H. Eliasson**, P. A. Andrekson "Four-span dispersion map optimization for improved nonlinearity mitigation in phase-sensitive amplifier links," Proceedings European Conference on Optical Communication (ECOC), Gothenburg, Sweden, 2017, paper P2.SC6.14

Acknowledgement

First of all I want to thank Prof. Peter Andrekson and Prof. Magnus Karlsson for their supervision and the opportunity to be a Ph. D. student at the photonics lab. It has been a great experience and I am glad to have been supervised by you. I also want to acknowledge Docent Pontus Johannison who got me into fiber-optics and played a large role in supervising me in the beginning of my Ph. D. studies.

A special thanks to Dr. Samuel Olsson for all the work and ideas put into our common projects. All the time we spent in the lab and out running was great fun. To Dr. Tobias Eriksson, my office mate for the first years of my Ph. D. studies, for learning me about all things related to fiber-optic communications. Those home brew evenings we arranged were truly memorable. To Dr. Abel Lorences-Riesgo for teaching me about all things related to fiber nonlinearities and the student project we collaborated on. I learned a lot from all of you.

To Sofie, you mean everything to me. To my son Erwin who considers it normal for dads to work with lasers. To my daughter Astrid who does not yet know how a laser works. To my parents Lena and Ingemar for always being there.

Henrik Eliasson

Göteborg
April 2018

This work was financially supported by the European Research Council Advanced Grant PSOPA (291618), the Swedish Research Council (VR) and the Knut and Alice Wallenberg Foundation (KAW). OFS Denmark is acknowledged for providing highly nonlinear fibers.

Abbreviations

ASE amplified stimulated emission
ASIC application-specific integrated circuit
AWG arbitrary waveform generator
AWGN additive white Gaussian noise
CD chromatic dispersion
CDR conjugate data repetition
CMA constant modulus algorithm
CW continuous wave
DAC digital-to-analog converter
DBP digital back-propagation
DCF dispersion compensating fiber
DCM dispersion compensating module
DRA distributed Raman amplification
DRB double Rayleigh backscattering
DSP digital signal processing
EDC electronic dispersion compensation
EDFA Erbium-doped fiber amplifier
ENOB effective number of bits
EVM error vector magnitude
FBG fiber Bragg grating
FEC forward error correction
FOPA fiber-optic parametric amplifier
FWM four-wave mixing
GDR group delay ripple
GMI generalized mutual information
GN Gaussian noise
GVD group velocity dispersion
HNLF highly nonlinear fiber
IQM IQ modulator
LO local oscillator
MI mutual information
MSSI mid-span spectral inversion
NF noise figure
NFT nonlinear Fourier transform
NLI nonlinear interference
NLPS nonlinear phase shift
NLSE nonlinear Schrödinger equation
OFDM orthogonal frequency division multiplexing
OOK on-off keying
OP optical processor
OPC optical phase conjugation
OSNR optical signal-to-noise ratio
PAM pulse-amplitude modulation
PBC polarization beam combiner/splitter
PC phase conjugation
PCTW phase-conjugated twin waves
PDL polarization dependent loss
PIA phase-insensitive amplifier
PLL phase-locked loop
PM polarization multiplexed
PMD polarization mode dispersion
PPLN periodically poled lithium niobate
PSA phase-sensitive amplifier
QAM quadrature amplitude modulation
QPSK quadrature phase-shift keying
RFL Raman fiber laser
RIN relative intensity noise
RPU Raman pump unit
RRC root-raised-cosine
RZ return-to-zero
SBS stimulated Brillouin scattering
SE spectral efficiency
SMF single-mode optical fiber
SNR signal-to-noise ratio
SPM self-phase modulation
SRS stimulated Raman scattering
SSFM split-step Fourier method
WDM wavelength-division multiplexing
XPM cross-phase modulation

Contents

Chapter 1

Introduction

The idea to use glass fibers with a core and cladding of slightly different refractive indices as the transmission medium for optical signals originates from an article by Kao and Hockham published in 1966 [1]. The invention of the optical fiber together with the first demonstration of a functioning laser by Maiman in 1960 [2] and later the semiconductor laser [3, 4] are maybe the most important inventions that still form the technological basis for any fiber-optic communication system. A later invention which also proved important is the Erbium-doped fiber amplifier (EDFA) by Mears et al. in 1987 [5] which allowed for broadband amplification of light removing the need for electrical repeaters in long communication links.

The first fiber-optic communication systems [6] used simple modulation formats like return-to-zero (RZ)-on-off keying (OOK) [7] and inline dispersion compensation with dispersion compensating fibers (DCFs) [8] or fiber Bragg gratings (FBGs) [9]. Later, systems also made use of wavelength-division multiplexing (WDM) to transmit several channels in one fiber at different wavelengths, something which was made possible by the invention of the EDFA. The current speed record for coherent long-haul links is more than 70 Tb/s over transoceanic distances in a single fiber [10]. Modern systems use more advanced modulation formats [11, 12] such as polarization multiplexed (PM)-quadrature phase-shift keying (QPSK) and PM-16-quadrature amplitude modulation (QAM). Laboratory demonstrations have been done with up to 4096-QAM [13]. Advanced links can also employ constellation shaping [14], soft-decision forward error correction (FEC) [15] and nonlinearity compensation [10] in order to achieve higher spectral efficiency (SE). The link itself usually contains fiber spans of 50-120 km length with EDFAs between fiber spans in order to recover the fiber loss. In the receiver, the signal is mixed with

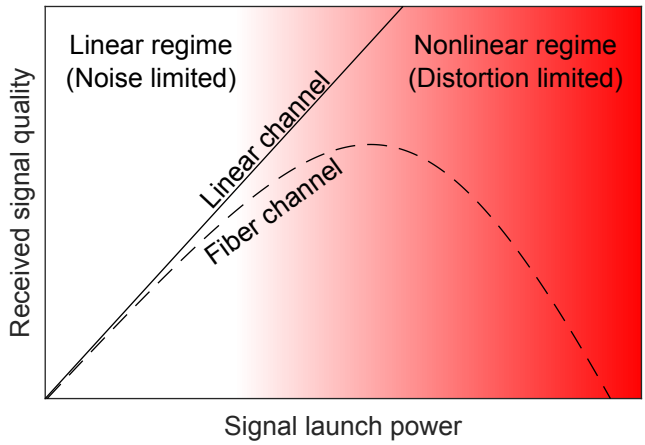

Figure 1.1: Received signal quality after propagation in an optical fiber as a function of signal power launched into the fiber.

a local oscillator (LO) laser in a 90 degree hybrid so that both the amplitude and phase of the optical signal can be detected. After detection the signal goes through digital signal processing (DSP) [16] that can e.g. remove the effect of chromatic dispersion (CD) [17] and track the relative phase drift between the transmitted signal and the LO laser.

On a fundamental level, the factors that limit the amount of information that can be reliably communicated over a fiber-optic communication link are the noise [18] added by the inline optical amplifiers [19] and the nonlinear distortion due to the Kerr effect [20] in the optical fiber itself. In order to reduce the impact of noise, one can increase the power of the light launched into the fiber. As the optical power is increased, the impact of the nonlinear distortion increases and eventually dominates over the noise meaning that the signal quality is made worse by further increasing the signal launch power. This is sometimes referred to as the nonlinear Shannon limit [21, 22]. This behaviour is also illustrated in Fig. 1.1. The two launch power regimes are often referred to as the linear and nonlinear regime. This behaviour at different launch powers leads to there being an optimum launch power that gives the best received signal quality. This optimum launch power lies in an intermediate regime where neither noise nor nonlinear distortion can be neglected. This intermediate regime is sometimes called the pseudo-linear regime [21]. This is in contrast to e.g. wireless communication systems where the transmission medium is air, which has negligible nonlinear properties.

Over the years, many methods have been suggested to mitigate the nonlin-

ear distortion due to the Kerr effect at high launch powers. The first method suggested was to use optical solitons in fiber-optic communication systems [23]. A soliton is an optical pulse that forms when the self-phase modulation (SPM) phase shift exactly counterbalances the group velocity dispersion (GVD). This leads to the pulse propagating unaltered in the fiber since the effects of dispersion and the Kerr effect cancel each other. This was a hot research topic in the 1990s but it was eventually found that such systems were not competitive because of e.g. soliton interaction [24] and the effect of Gordon-Haus jitter [25].

The second method suggested for compensating nonlinear distortion was optical phase conjugation (OPC) by Fisher et al. in 1983 [26]. In that paper, it was shown analytically, that by performing an OPC operation on the signal at the center point of a fiber-optic link, it is possible to undo the nonlinear distortion generated in the first half of the link by propagating the phase-conjugated signal through the second half of the link. This method was later experimentally demonstrated in [27]. In recent years there has been a renewed interest in the topic with the investigation of OPC links employing distributed Raman amplification and/or several inline OPC devices [28–31].

Both the use of solitons and OPC would qualify as all-optical approaches as clever optical designs and effects are used to reduce the impact of nonlinear distortion. Another group of methods are digital approaches where the compensation for nonlinear distortion is done in the digital domain in the transmitter or receiver. One digital method which has received significant attention in the research community over the last ten years is digital back-propagation (DBP). DBP was first suggested by Essiambre et al. in 2005 [32]. The idea behind DBP is to propagate the received optical field backward through the fiber by a brute force numerical solution of the nonlinear partial differential equation describing light propagation in an optical fiber. DBP has been a "hot" research topic ever since its introduction due to the potential for significant performance gains [33]. There are two big problems associated with the use of DBP, first, the complexity of the numerical calculations required is immense [34], second, in order to back-propagate a whole WDM spectrum we need to detect all channels simultaneously. In recent years there has been progress on the topic in several directions, e.g. with pre-distortion of several WDM channels simultaneously at the transmitter side [35, 36] or with DBP of several WDM channels with the use of a spectrally sliced coherent receiver [37]. Even compensation for the interactions between nonlinear effects and polarization mode dispersion (PMD) has been investigated by taking the average PMD into account in the backpropagation algorithm [38].

When discussing digital methods one should also mention the use of the nonlinear Fourier transform (NFT) [39–41]. The idea is to encode information on the NFT which is a mathematical construct unaltered by propagation over a nonlinear fiber channel in contrast to the time domain representation

of the waveform which could be severely distorted. One implementation is to calculate a data-carrying NFT at the transmitter side and transmit the signal modulated on laser light. The NFT of the waveform is unaltered by the propagation over fiber and at the receiver side the NFT is reversed for retrieval of the data undistorted by fiber nonlinearities. Even though this solution seems elegant it suffers from many similar problems as DBP. It is e.g. very computationally demanding to calculate the NFT [42] and much more work is needed in this area to realize the full potential of the technique.

A fifth method that was proposed recently is phase-conjugated twin waves (PCTW) [43]. The idea behind this concept is to transmit a phase-conjugated copy of the signal alongside the signal on the orthogonal polarization. In the receiver DSP, the two fields are coherently superposed leading to mitigation of nonlinear distortion if certain conditions are fulfilled. This concept was also generalized to utilize other signalling dimensions than polarization for the phase-conjugated copy in [44]. In [45], a modification of PCTW in order to improve SE was investigated and in [46], a PCTW subcarrier coding scheme was investigated in an orthogonal frequency division multiplexing (OFDM) system. A scheme with similarities to PCTW that transmitted the phase-conjugated copy on a separate wavelength followed by coherent superposition in DSP was investigated in [47].

The sixth method which will be discussed here is to use the two-mode copier-phase-sensitive amplifier (PSA) scheme. This has been shown to offer improved performance in a nonlinear transmission regime [48] as well as in a linear regime because of their 0 dB quantum limited noise figure (NF) [49]. There are similarities between the use of two-mode PSAs and the concept of PCTW since in both cases, a phase-conjugated copy is transmitted alongside the signal. An important difference between PCTW and a PSA link is that the coherent superposition operation is performed all-optically in a PSA link, opening up the possibility to perform the coherent superposition inline at each amplifier site. Both the OPC and copier-PSA scheme can provide distributed nonlinearity compensation which can be advantageous in terms of e.g. nonlinear signal-noise interaction [29]. Another method for providing distributed nonlinearity compensation is the use of intensity-directed optoelectronic circuits, this was investigated in [50].

All of these methods have been experimentally demonstrated and shown to improve the tolerance to nonlinear distortion. It is however important to point out that the majority of these methods, with the possible exception of compensation of nonlinearities in the digital domain, are not available in commercial products. There are commercial products that claim to use nonlinearity compensation in the digital domain [51], but it is at the moment unclear exactly how it is implemented and what kind of performance gains that can be achieved. The reason for the other methods not being used in commercial

communication systems are different for each method but in general one can say that the performance gain does not yet outweigh the increased system complexity and cost. In the case of OPC, the optical complexity of the link itself is significantly increased because of the inline OPC devices. If using DBP based on the split-step Fourier method (SSFM), the required computation power at the receiver side is too high [33] to be feasible with todays semiconductor technology even though this could change as application-specific integrated circuit (ASIC) technology and algorithms improve [Paper K]. In the case of PCTW it is different since it is not the question of complexity which is stopping the method from being used. Instead, it is the fact that the SE of the system is reduced by 50 % due to the transmission of the phase-conjugated copy. In most cases it is not acceptable to reduce SE by 50 % compared to e.g. PM-QPSK. The research on long-haul links using PSAs is still in its early stages but it is clear that system complexity is an issue in such systems as well on top of the reduced SE. In order for all-optical nonlinearity mitigation methods to become attractive in fiber-optic communication systems it is important to reduce cost/complexity as well as understand and optimize the mitigation of nonlinear distortion.

1.1 This thesis

The work presented in this thesis is focussed on nonlinearity compensation techniques based on the idea to transmit a phase-conjugated copy alongside the signal. There are many possible implementations of this general concept and in the appended papers we study two different implementations. The first implementation is studied in [Paper A] where the time domain is chosen as the signalling dimension for the phase-conjugated copy. The rest of the appended [Papers B-F] investigate different aspects of nonlinearity mitigation using the two-mode copier-PSA scheme where the phase-conjugated copy is transmitted on another wavelength. The focus in this thesis is on the understanding and optimization of the nonlinearity mitigation properties of such links.

Thesis outline

Chapter 2 begins with a general description of what we mean by linear and nonlinear fiber propagation effects followed by detailed descriptions of these effects. This is followed by a overview of distributed Raman amplification (DRA), which is used in [Paper C] and [Paper F], and a description of the numerical and theoretical methods used to analyze the effects of fiber nonlinearities. Chapter 3 contains descriptions of the different optical signal processing devices that are used in the two-mode copier-PSA scheme as well as the OPC scheme. In Chapter 4 we discuss and derive the different all-optical

nonlinearity mitigation methods. Special attention is given to the copier-PSA scheme which is the topic of most the appended papers. In Chapter 5 there is a discussion on possible future directions of research in the same or closely related research areas.

Chapter 2

Light propagation in fibers

The physical effects that alter the optical field during propagation in an optical fiber are commonly divided into linear effects such as attenuation and dispersion, and nonlinear effects due to the Kerr effect as well as Raman and Brillouin Scattering. At low optical power, the nonlinear effects can be neglected and the evolution of the field is well described by linear effects. As the optical power of the field is increased, the nonlinear effects become stronger and will at high enough powers distort the signal beyond recognition. Linear and nonlinear effects will be discussed separately below.

First we provide a short explanation of what we mean by linear and nonlinear effects in fiber optics. We start by going back to mathematical definitions. A mathematical function or operator F is said to be linear if

$$F(\alpha x + \beta y) = \alpha F(x) + \beta F(y). \tag{2.1}$$

This means that $F(\beta y)$ is independent of the variable x as well as linearly proportional to the constant β. If Eq. 2.1 does not hold, the function is said to be nonlinear. In the context of fiber optics, x and y could be e.g. neighbouring wavelength channels and F the transfer function of an optical fiber. At low optical powers Eq. 2.1 will model a fiber optic channel well. At high optical powers the output from y will also depend on x and the system is then called nonlinear.

2.1 Linear fiber effects

As a lightwave propagates in an optical fiber, power is lost, mainly due to material absorption and Rayleigh scattering. The evolution of the optical

power $P(z)$ in the presence of linear attenuation is governed by Beer's law and can be written as

$$P(z) = P(0)\exp(-\alpha z), \tag{2.2}$$

where α is the attenuation coefficient. For modern optical fibers designed to achieve low attenuation, α is typically below 0.17 dB/km at 1550 nm [52], meaning that less than 4 % of the light is lost per km. Associated with the attenuation, the effective length is defined as

$$L_{\text{eff}} = \frac{1}{\alpha}(1 - \exp(-\alpha L)), \tag{2.3}$$

where L is the length of the fiber. For a long standard single-mode optical fiber (SMF), the effective length is approximately 21 km. The physical meaning of the effective length is the length over which the accumulated nonlinear phase shift

$$\phi_{\text{NL}}(z) = \gamma \int_0^z P(z')dz', \tag{2.4}$$

where γ is the nonlinear coefficient [1/(W km)], equals $\phi_{\text{NL}}(L) = \gamma L_{\text{eff}} P(0)$, i.e. the length over which a constant optical power gives the same ϕ_{NL}. Light of different wavelength propagate with different group velocities in an optical fiber. This is referred to as group velocity dispersion (GVD) or chromatic dispersion (CD). Linear propagation of an optical field is described in frequency domain by

$$\tilde{E}(z,\omega) = \tilde{E}(0,\omega)\exp(i\beta(\omega)z), \tag{2.5}$$

where $\beta(\omega)$ is the propagation constant. The real part of β describes dispersive properties while the imaginary part describes attenuation. In order to analyze the frequency dependence of the propagation constant, $\beta(\omega)$ is Taylor expanded around the carrier frequency ω_0 according to

$$\beta(\omega) = \beta_0 + \beta_1(\omega - \omega_0) + \frac{\beta_2}{2}(\omega - \omega_0)^2 + \frac{\beta_3}{6}(\omega - \omega_0)^3 + ..., \tag{2.6}$$

where β_1 is the group velocity at the carrier frequency, β_2 the GVD coefficient and β_3 describes the frequency dependence of the GVD. The GVD coefficient is given in units of [ps^2/km] and is related to the dispersion parameter $\mathrm{D} = -2\pi c\beta_2/\lambda^2$ which is given is units of [ps/(nm km)].

Yet another linear propagation effect is PMD which is due to the randomly varying birefringence of the optical fiber. The random birefringence of subsequent segments of an optical fiber is due to non-uniformities in fabrication, e.g. deformed core geometry, fiber stress or bending. This leads to pulse spreading through frequency dependent polarization rotations during propagation. This effect is often neglected in computer models of nonlinear propagation of light in a fiber, not because it is not important but because of the increased complexity due to having to deal with statistical analysis on a large collection of random fibers.

2.2 Nonlinear fiber effects

The Kerr effect, discovered by scottish physicist John Kerr in 1875 [53, 54], is a change in the refractive index of any material when an electromagnetic field is applied. At a more fundamental level this is due to the nonlinear polarization response of the material. This effect is commonly described by introducing a intensity-dependent part n_2 of the refractive index

$$n(\omega, P) = n_0(\omega) + n_2(P/A_{\text{eff}}) \tag{2.7}$$

where P is the optical power, n_2 is the nonlinear-index coefficient and A_{eff} is the effective area of the fiber mode. The strength of the nonlinearity in a fiber is specified by the nonlinearity coefficient

$$\gamma = \frac{2\pi n_2}{\lambda A_{\text{eff}}}, \tag{2.8}$$

where λ is the wavelength of the light. Nonlinear propagation of light in an optical fiber is commonly modeled using the two coupled equations of the Manakov model [55]

$$\frac{\partial E_{\text{X}}}{\partial z} = -\frac{i\beta_2}{2}\frac{\partial^2 E_{\text{X}}}{\partial t^2} + \frac{g(z)-\alpha(z)}{2}E_{\text{X}} + i\gamma(|E_{\text{X}}|^2 + |E_{\text{Y}}|^2)E_{\text{X}}, \tag{2.9}$$

$$\frac{\partial E_{\text{Y}}}{\partial z} = \underbrace{-\frac{i\beta_2}{2}\frac{\partial^2 E_{\text{Y}}}{\partial t^2}}_{\text{dispersion}} \underbrace{+\frac{g(z)-\alpha(z)}{2}E_{\text{Y}}}_{\text{local loss/gain}} + \underbrace{i\gamma(|E_{\text{X}}|^2 + |E_{\text{Y}}|^2)E_{\text{Y}}}_{\text{nonlinearities}}, \tag{2.10}$$

where E_{X} and E_{Y} are proportional to the electrical fields of two orthogonal polarization states and $g(z)$ and $\alpha(z)$ are the local gain and attenuation. In these equations higher-order dispersive effects due to β_3 as well as the effect of Raman and Brillouin scattering have been neglected. One can however point out that e.g. the gain from distributed Raman amplification still can be modeled by Eqs. (2.9) and (2.10) through the parameter $g(z)$. The last term in the equations is what gives rise to nonlinear effects.

2.3 Lumped amplification

Associated with the loss is the need to recover losses through amplification. This inevitably leads to the addition of noise. If we recover the losses using a lumped optical amplifier with gain G, noise is added to the signal with a power spectral density of [56]

$$S_{\text{ASE}}(\nu) = \eta_{\text{sp}} h\nu_0 (G-1) \tag{2.11}$$

where η_{sp} is the spontaneous emission factor, h the Planck constant and ν_0 is the frequency of the light. Associated with this, the NF is defined as the ratio between the input signal-to-noise ratio (SNR) and the output SNR as [56]

$$\text{NF} = \frac{\text{SNR}_{\text{in}}}{\text{SNR}_{\text{out}}} \approx 2\eta_{\text{sp}}, \tag{2.12}$$

valid in a high gain regime. For any optical amplifier where the gain is insensitive to the phase of the incoming light the quantum-limited NF is 3 dB [57–59]. Later in section 2.4.1 we will expand the concept of NF to the distributed amplification case.

2.4 Distributed Raman amplification

Raman scattering, named after physicist Chandrasekhara Raman [60] is an inelastic scattering process meaning that the scattered light has a different frequency than the incoming light. An important application of Raman scattering in fiber-optic communication systems is distributed Raman amplification [61]. In a fiber span with distributed Raman amplification, the signal propagates in the transmission fiber together with one or more pump waves and power is transferred from the pump waves to the signal through stimulated Raman scattering (SRS). In this manner it is possible to improve noise properties with the use of distributed Raman amplification since the local optical signal power in the later parts of the span is higher relative to the added noise. For example, in a 100 km span, the span NF can be improved by 6 dB compared to a EDFA-amplified span through the use of backward pumped Raman amplification [62, Table 3.1], more on this in the next section. Transmission over long single hop links is one application where DRA can provide great benefits by providing distributed gain[63]. The pump waves can be copropagating, counterpropagating or both with two or more pump waves, more on this in section 2.4.2. The Raman gain that the signal experiences depends on e.g. the wavelength separation between the signal and the pump and the pump power. In regular SMF, the peak in the Raman gain spectrum is located at frequency shifts around 13.2 THz, meaning that in order to amplify a signal at 1550 nm, the pump should be located around 1450 nm [62, Chapter 1.2].

The local gain due to DRA in a span of length L, $g(z)$ in Eqs. 2.9 and 2.10, can be expressed e.g. in the case of a single backward pump as

$$g(z) = \sqrt{g_R P_0 \exp(-\alpha_p(L-z))}, \tag{2.13}$$

where g_R is the Raman gain coefficient, P_0 the Raman pump power and α_p the loss at the pump wavelength. Note that we define $g(z)$ in amplitude domain.

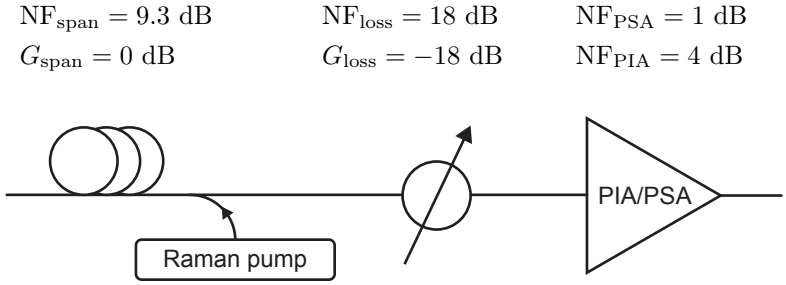

Figure 2.1: Simplified model used to estimate the equivalent span NF of the hybrid PSA-DRA link in [Paper F]. The example numbers in the figure are taken from [Paper F].

By integrating the square of the local gain over the span we get the expression for the net power gain in a span of length L as

$$G_R = \exp\left(g_R \int_0^L P_0 \exp(-\alpha_p(L-z))dz - \alpha L\right), \tag{2.14}$$

The reason why distributed Raman amplification is interesting in the context of mitigation of nonlinear fiber distortion with all optical methods, e.g. using OPC or PSAs, is because it is the most straightforward way of manipulating the span power map. In the case of OPC, it has long been known that in order to optimize the mitigation of nonlinear distortion, a symmetric power map around the OPC point is needed [26]. In the case of PSAs, it was shown in [Paper C] that the inline mitigation of nonlinear distortion through coherent superposition in PSAs could become more efficient by also using distributed Raman amplification.

2.4.1 Equivalent span noise figure

In [Paper F] we provided simple analytical estimates of the equivalent span NF for the different investigated amplifier configurations. The equivalent span NF is often defined as the total NF of the cascade of all components in the span. In this section we will expand on this and provide more details on how these calculations are performed. We discuss how to estimate the equivalent span NF of a link combining DRA and PSAs taking the lumped losses due to PSA specific components into account. This could also be used to make estimations on the trade-off between increased span loss and improved nonlinearity mitigation due to inline dispersion compensation in copier-PSA links, more on this in section 4.4.1.

We start by presenting the equivalent NF of a span of length L with backwards Raman pumping [64, Eq. (3.2.3)]

$$\mathrm{NF}_{\mathrm{R,back}} = 1 + 2\frac{\eta_{\mathrm{sp}}\alpha}{g_r(P_p)^L}(G_R - 1) \tag{2.15}$$

where η_{sp} is the spontaneous scattering factor, the loss α is assumed to be the same at the signal and pump wavelength, g_r the Raman gain coefficient, P_p the Raman pump power and G_R the Raman on-off gain. If we assume a 0 dB span net gain we get $G_R = \alpha L$. To get such a simple closed form expression one must approximate that the loss at the Raman pump wavelength and the signal wavelength is the same. In the simulations in [Paper C] we used the theoretical concept of ideal DRA. By this we mean distributed amplification where the loss is exactly counterbalanced by DRA gain at every point in the fiber. In this case the equivalent NF can be further simplified to

$$\mathrm{NF}_{\mathrm{R,ideal}} = 10\log(2\alpha_s L + 1), \tag{2.16}$$

where α_s is the loss at the signal wavelength. This is of course not possible in practice but using the techniques discussed in section 2.4.2 it is possible to get remarkably close.

In Fig. 2.1 we illustrate the simplified model that was used to estimate the equivalent span NF with example values of loss and NFs taken from [Paper F]. The cascade consists of a span with ideal DRA giving a net gain of 0 dB and a NF of 9.3 dB followed by a lumped loss of 18 dB and a PSA or phase-insensitive amplifier (PIA) with a 1 or 4 dB NF. Using Friis formula [65] we get an expression for the equivalent span NF

$$\mathrm{NF}_{\mathrm{eq}} = \mathrm{NF}_{\mathrm{span}} + \frac{(\mathrm{NF}_{\mathrm{loss}} - 1)}{G_{span}} + \frac{\mathrm{NF}_{\mathrm{PSA}} - 1}{G_{\mathrm{loss}}}. \tag{2.17}$$

Note that all quantities are specified in linear units in the above expression. When calculating this expression with the example values we get an equivalent NF of 19.4 dB. Compare this to the NF of only the loss and the PSA which is 19 dB and it becomes clear that the dominating noise source in the example is the lumped loss. Taking the losses from inline dispersion compensation into account could be done with this approach as well.

2.4.2 Advanced distributed Raman amplification schemes

There are several ways of using distributed Raman amplification, the least complex is to have a single backward pump in the transmission fiber which is what was used in [Paper C] and [Paper F]. In this way it is possible to have local gain in the latter parts of each transmission fiber. As a consequence,

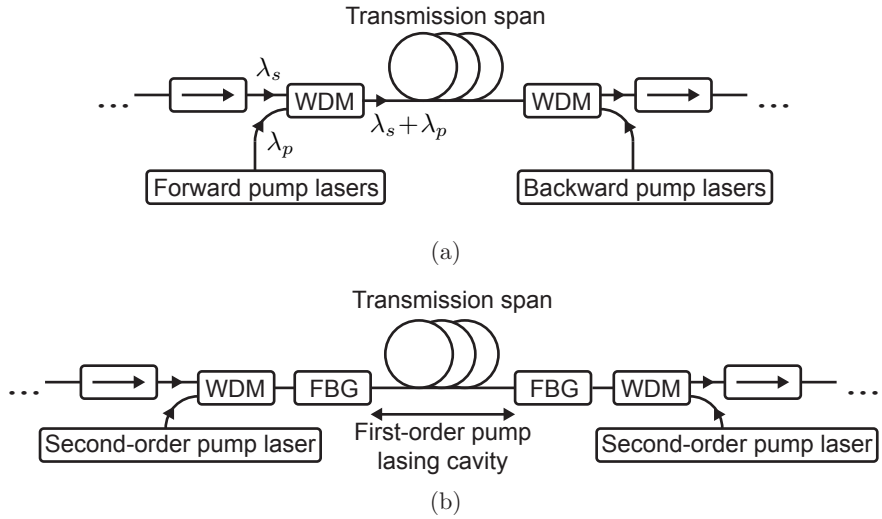

Figure 2.2: Illustration of advanced distributed Raman amplification schemes. (a) Bidirectional pumping scheme: The signal at wavelength λ_s is combined with the forward pump at wavelength λ_p into the fiber span with a WDM-coupler. At the end of the span, a pump is coupled in the backward direction into the fiber span with a second WDM-coupler. Optical isolators are placed before and after each span to stop Rayleigh backscattered light from accumulating over many spans. Pumps at several wavelengths as well as higher-order pumps can be used in both directions to increase gain bandwidth and power map flatness. (b) Raman fiber laser scheme: Second-order pumps are coupled into the span, possibly in both directions. The FBGs are reflective at the first-order pump wavelength creating a laser cavity for the first-order pump. Lasing starts at the first-order pump wavelength which then provides gain for the signal.

the equivalent span NF is reduced and the span power map is altered. In the context of all-optical nonlinearity mitigation, having a flat span power map can vastly improve the efficiency of the nonlinearity mitigation. In the experiment presented in [Paper F] we used a DRA pumping scheme where we divided the span into three segments and pumped each of the segments individually. In a lab environment this can be done but in real systems it is not feasible since that would require placing active optical components inside each transmission span. In the paper we argued that there are realistic schemes that can achieve a similarly flat or symmetric span power map without any active components inside the transmission span. Here follows a quick review and discussion of

the techniques that could be used.

If the purpose is to achieve a symmetric or flat power map, pumps propagating in both the backward and forward direction can be used [66]. Yet another technology that can be used to achieve flatter span power maps with DRA is higher-order pumping. Higher-order pumping refers to the use of pumps that amplify the first-order pump, leading to the first-order Raman pump experiencing distributed gain and providing a more evenly distributed gain to the signal. In [67], second-order bidirectional pumping was used to realize a 80 km Raman amplified span with power excursions of only ± 0.4 dB. A sketch of a bidirectionally pumped transmission span is shown in Fig. 2.2(a).

Second-order pumps can also be used in a Raman fiber laser (RFL) based scheme where FBGs with high reflectivity at the first-order pump wavelength are placed at both ends of each span leading to a first-order pump being generated in a manner similar to lasing [68]. Such RFL amplification was demonstrated in [69]. Also worth noting is that the generated lasing could be achieved in both a random lasing mode as well as a Fabry-Perot cavity lasing mode in the transmission fiber. Nice features of the RFL scheme are that relatively large optical gain bandwidths as well as a relatively flat span power map can be achieved without having several second-order pumps at different wavelengths. The RFL scheme is illustrated in Fig. 2.2(b).

Going back to the experiment presented in [Paper F], both the RFL scheme and bidirectional higher-order pumping could be used to achieve similar levels of power map flatness as in the experiment but without placing any active components inside the transmission span. It is however not clear at the moment which DRA scheme which is most suited for systems employing all-optical nonlinearity mitigation. A comparison between different DRA schemes in copier-PSA links is beyond the scope of this thesis.

2.4.3 Relative intensity noise and Rayleigh scattering

In this section we will discuss two physical effects, relative intensity noise (RIN) and Rayleigh scattering, which can give significant penalties in systems striving for a flat power map using DRA. A flat power map is often desired in links with all-optical nonlinearity mitigation using e.g. OPC devices or PSAs.

First we discuss RIN [70, Chapter 5.5] of the pump laser transferring onto the signal. Since the Raman gain depends on the Raman pump power exponentially, see Eq. 2.14, it is reasonable to believe that amplitude fluctuations on the pump will create large amplitude fluctuations on the signal. If the Raman pump is travelling in the forwards direction this will lead to significant penalties since the RIN of the pump wave will transfer efficiently onto the signal when they are copropagating [71]. In recent years this was further investigated in [72] where limits on the acceptable levels of RIN in unrepeatered systems

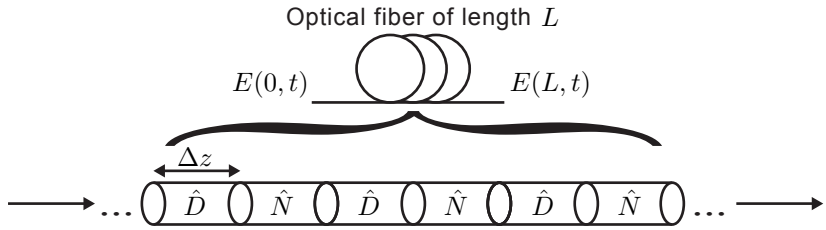

Figure 2.3: Illustration of the SSFM, the fiber length L is divided into several segments of length Δz and the field $E(0,t)$ is propagated alternating between linear steps according to Eq. (2.18) and nonlinear steps according to Eq. (2.19) in order to find the solution $E(L,t)$.

was investigated for different modulation formats. For the RFL scheme, it was found in [69] that the limiting factor to system performance was RIN transfer from copropagating pumps.

Another phenomenon that could become important in systems with highly efficient nonlinearity mitigation as well as DRA is Rayleigh scattering [73]. In spans with high distributed gain, i.e. span transparency or net gain, the light which is scattered backwards in the fiber through Rayleigh scattering is amplified and can be scattered again into the forwards direction, this is called double Rayleigh backscattering (DRB) [74, 75]. This also happens for the backwards travelling amplified stimulated emission (ASE) due to DRA which can be scattered into the forwards direction. The light in the forwards direction originating from DRB of the signal will appear as noise with a similar spectral profile as the signal. If the DRB from the signal is dominating over the backwards travelling ASE scattered into the forwards direction the power of the DRB light depends linearly on the signal power, i.e. increasing the signal power by 1 dB also increases the DRB light power by 1 dB. As a result DRB light originating from the signal will dominate over ASE at sufficiently high signal power levels. In regular coherent fiber optic communication systems this effect can usually be neglected but this is not necessarily the case when studying systems employing all-optical nonlinearity mitigation which could have high optimal signal launch powers.

2.5 Split-step Fourier method

The most commonly used method for computer modelling of light propagation in a fiber is the split-step Fourier method (SSFM) [76]. The basic idea behind the method is to divide each step ∂z of Eqs. (2.9) and (2.10) into two parts,

one step propagating with linear effects, dispersion and attenuation and one nonlinear step applying an SPM rotation. The linear step is described by the operator [62, Chapter 2.4.1]

$$\hat{D} = -\frac{i\beta_2}{2}\frac{\partial^2}{\partial t^2} + \frac{g(z) - \alpha(z)}{2} \tag{2.18}$$

with the same definitions of parameters as in Eq. 2.9 and 2.10. while the nonlinear step is described by the operator

$$\hat{N} = i\gamma(|E_{\mathrm{X}}|^2 + |E_{\mathrm{Y}}|^2). \tag{2.19}$$

The propagation is then performed in steps of length Δz according to

$$E_{\mathrm{X,Y}}(z + \Delta z, t) \approx \exp(\Delta z \hat{D}) \exp(\Delta z \hat{N}) E_{\mathrm{X,Y}}(z, t) + n(z, t), \tag{2.20}$$

where the two operators are evaluated consecutively, the linear operator in frequency domain and the nonlinear operator in time-domain. The noise term $n(z, t)$ represents noise from distributed amplification, e.g. DRA. The noise term is often approximated as a additive white Gaussian noise (AWGN) process with variance [64, Chapter 2.2.1]

$$\sigma^2 = n_{\mathrm{sp}} h \nu_0 g_R P_p(z), \tag{2.21}$$

where n_{sp} is the spontaneous Raman scattering factor, g_R is the Raman gain coefficient and $P_p(z)$ is the local Raman pump power. In the simplest case of backward pumped DRA, $P_p(z) = P_0 \exp(-\alpha_p(L - z))$, where α_p is the loss at the Raman pump wavelength. The spontaneous Raman scattering factor is calculated as [64, Chapter 2.1.3]

$$n_{\mathrm{sp}} = \frac{1}{1 - \exp(-h\Omega/k_B T)}, \tag{2.22}$$

where Ω is the Raman shift, k_B is the Boltzmann constant and T the temperature of the fiber. We see that the noise levels added by DRA is dependent both on the Raman shift Ω which is material dependent and on the temperature T of the transmission fiber. Of course, in reality the linear and nonlinear effects occur simultaneously and not in a consecutive manner. Because of this it is important to choose the step-size Δz carefully in order to obtain an accurate approximation of Eqs. (2.9) and (2.10) using the SSFM [77]. The idea behind the SSFM is illustrated in Fig. 2.3.

In this thesis, the main application of the SSFM is to evaluate the optical field after propagation in an optical fiber with the purpose of estimating the performance of different schemes for nonlinear distortion mitigation. Another important application of the SSFM that should be mentioned is DBP [33]

which is the idea to propagate the optical waveform backwards through the fiber in digital domain using the SSFM. Although there are other ways of propagating the received optical field backward through the fiber, DBP based on SSFM is often considered as a reference when benchmarking alternative methods that can be based on e.g. a perturbation approach [78], Volterra series [79, 80] or stochastic DBP [81]. As was mentioned in the introduction, the main problem with using the SSFM for the purpose of DBP is the computational complexity and both of these alternative approaches are used in an attempt to reduce complexity.

2.6 Perturbation theory

Perturbation theory is a useful tool for theoretical analysis of nonlinear distortion in the weakly nonlinear regime. Perturbation theory is based on the assumption that

$$|\delta_{NL}| \ll |E_S|, \tag{2.23}$$

where $|\delta_{NL}|$ is the amplitude of the nonlinear distortion and $|E_S|$ is the amplitude of the signal. Under this assumption, the nonlinear distortion δ_{NL} is generated by a source field E_S propagating only taking β_2 and α into account. These assumptions also make it possible to do analytical calculations of the nonlinear distortion generated by e.g. a Gaussian pulse train [82]. Perturbation theory can be used e.g. to make a first-order theory for the mitigation of nonlinear distortion for some of the methods discussed in this thesis. This has been done for the case of PCTW in [43] with a frequency domain perturbation analysis and for the case of conjugate data repetition (CDR) in [Paper A] with a time domain perturbation analysis. In the frequency domain analysis, the spectrum of the nonlinear distortion $\tilde{\delta}_{NL}(\omega)$ is calculated, while in the time domain analysis, the time domain representation $\delta_{NL}(t)$ is calculated.

In section 4.4, the frequency domain perturbation analysis will be used to derive the nonlinear distortion mitigation properties of a single-span PSA link. An important aspect to point out about these derivations is that since they are based on a perturbation theory, they are formally not valid in a highly nonlinear regime, i.e. when $|\delta_{NL}|$ cannot be neglected compared to $|E_S|$. The derivations can not safely predict what will happen and how well nonlinear distortion will be mitigated in a strongly nonlinear regime. The best approach for evaluating performance in a strongly nonlinear regime is to perform numerical simulations using the SSFM or by performing experiments.

Another important application of perturbation theory in recent years is the development of the Gaussian noise (GN) model [83]. The basic idea behind the GN model is to apply perturbation theory in order to find the nonlinear distortion generated in a highly dispersive regime. The conclusion of that work

is that under certain assumptions, reasonably valid for modern coherent fiber-optic communication systems, the nonlinear distortion will appear as AWGN even though the nonlinear distortion is deterministic. The GN model has proven to be very successful in predicting nonlinear interference (NLI) and system performance in general in typical coherent dispersion uncompensated WDM links. The GN model was later extended to improve accuracy in the first few spans of a fiber-optic link where the signal statistics are not Gaussian. In [84, 85] the GN model was extended to account for DRA.

Now, a solution of Eq. (2.9) based on a single-polarization frequency domain perturbation analysis will be presented. This solution will be used in section 4.4 in the derivation of the mitigation of nonlinear distortion in a single-span PSA link. We start by expanding Eq. (2.5) with a first-order nonlinear perturbation term $\tilde{u}^{(1)}(z,\omega)$ according to [86]

$$\tilde{E}(z,\omega) = \sqrt{P_0}\exp\left(\frac{G(z)+iC(z)\omega^2}{2}\right)\left[\tilde{u}^{(0)}(\omega)+\tilde{u}^{(1)}(z,\omega)\right], \tag{2.24}$$

where P_0 is the average launch power and $\tilde{u}^{(0)}(\omega)$ is the transmitted signal spectrum normalized such that $< |u^{(0)}(t)|^2 >= 1$. The logarithmic power evolution $G(z)$ is given by

$$G(z) = \int_0^z [g(z') - \alpha(z')]dz', \tag{2.25}$$

where $\alpha(z)$ is the local attenuation and $g(z)$ is the local gain which can be achieved by e.g. Raman amplification. The expression for the accumulated dispersion is

$$C(z) = \int_0^z \beta_2(z')dz'. \tag{2.26}$$

The expression for the first-order perturbation term is then [86]

$$\begin{aligned}\tilde{u}^{(1)}(L,\omega) = i\gamma P_0 L_{\text{eff}} \int_{-\infty}^{\infty} \mathrm{d}\omega_1 \int_{-\infty}^{\infty} \mathrm{d}\omega_2 \eta(\omega_1,\omega_2) \\ \times \tilde{u}^{(0)}(\omega+\omega_1)\tilde{u}^{(0)}(\omega+\omega_2)\tilde{u}^{(0)*}(\omega+\omega_1+\omega_2),\end{aligned} \tag{2.27}$$

where $\eta(\omega_1,\omega_2)$ is the nonlinear transfer function [86]

$$\eta(\omega_1,\omega_2) = \frac{1}{L_{\text{eff}}}\int_0^L \exp[G(z) - i\omega_1\omega_2 C(z)]dz, \tag{2.28}$$

which fully defines the nonlinear properties of the link in the first-order approximation. In order to have a more intuitive understanding of Eq. (2.27), one can interpret the double integral over ω_1 and ω_2 as the calculation of all

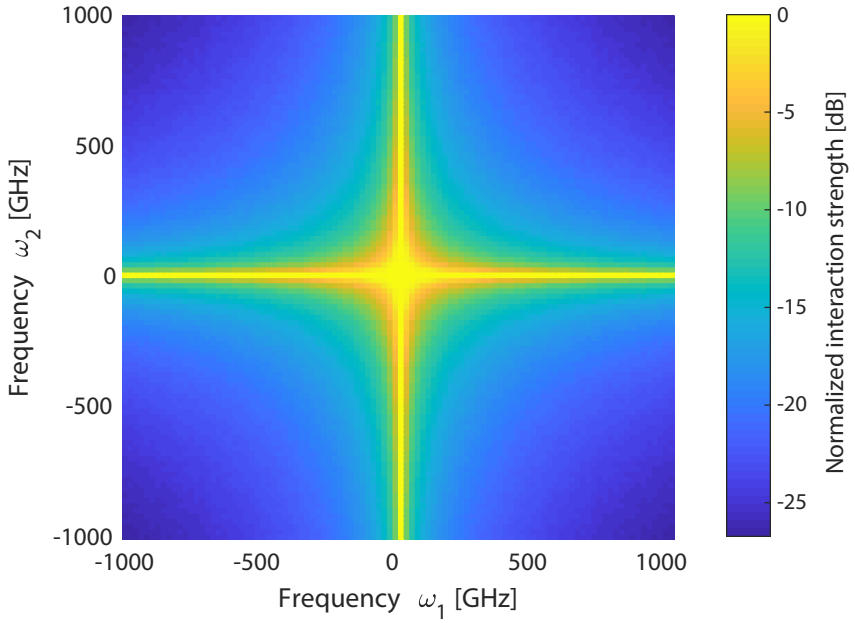

Figure 2.4: The FWM strength as a function of the frequency of the interacting components ω_1 and ω_2 according to Eq. 2.28. The interaction strength has been normalized. The calculation was done for a single span with parameters $L = 80$ km, $D = 17$ [ps/nm/km] and $\alpha = 0.2$ [dB/km].

four-wave mixing (FWM) terms for which the FWM product end up at ω. An illustration of the nonlinear transfer function $\eta(\omega_1, \omega_2)$ is shown in Fig. 2.4. Worth noting here is also that this perturbation model does not take into account ASE noise from optical amplifiers, in the regime where a perturbation model is valid this is often a good approximation however. The expression for the nonlinear perturbation, Eq. (2.27), is very general and can be used for many purposes other than deriving the mitigation of nonlinear distortion in PSA links which will be done in section 4.4. Eq. (2.27) is also the starting point in the derivation of the GN model [83].

Chapter 3

Optical signal processing

In this chapter we will introduce the basics of the optical signal processing techniques that are used to enable nonlinearity mitigation in OPC and copier-PSA links. We divide this into two parts, first a discussion on phase conjugation which is used in OPC links and the copier stage of a copier-PSA link. Second, we discuss the optical signal processing capabilites of two-mode PSAs. All of this will later be used in Chapter 4 in the context of fiber nonlinearity mitigation.

3.1 Optical phase conjugation

The first suggested application of phase conjugation in fiber-optic communication systems was dispersion compensation. In 1979, Yariv et al. showed analytically that by performing OPC using FWM on a pulse in the center point of a fiber-optic link, the effects of dispersion due to β_2 in the first half of the link can be reversed and the pulse is returned to its original shape after propagation over the second half of the link [87]. The process of performing OPC once at the centerpoint of a link is sometimes also referred to as mid-span spectral inversion (MSSI). This was long before the age of coherent detection with CD compensation in DSP and the issue of how to perform dispersion compensation all-optically was an open question and OPC was considered as a possible option.

The next big step in the study of OPC in fiber optics came in 1983 when Fisher et al. showed that when performing MSSI, not only are the effects due to CD cancelled, but it is also possible to compensate for the combined effect of CD and SPM due to the Kerr effect [26]. A brief theoretical explanation of the reversal of GVD and SPM will be provided in section 4.1. Since then, the study

of OPC in fiber optics has been an ongoing topic, being popular in the 1990s, with experimental studies of the polarization dependence of OPC devices [88, 89], CD compensation [90] and numerical studies of nonlinearity mitigation [91, 92]. In the 2000s, OPC in WDM systems was studied numerically [93] and in experiments [94]. In recent years, fiber-optic communication systems using both distributed Raman amplification and OPC [30, 31, 95] as well as systems employing several inline OPC devices [28, 29, 31] have received attention. These topics will be discussed more in section 4.1.

Another way that phase conjugation can be used in order to mitigate nonlinear distortion is to generate a phase-conjugated copy of the signal wave at the transmitter and transmit both waves alongside each other. By performing coherent superposition of the waves it is then possible to mitigate nonlinear distortion due to the Kerr effect [43]. This method has received attention in recent years with demonstrations of mitigation of nonlinear distortion in copier-PSA [48] and PCTW [43] links. These topics will be discussed in sections 4.2, 4.3 and 4.4.

One can also mention that the process of phase conjugation (PC) is not unique for lightwaves. It is also possible to perform PC on e.g. acoustic waves [96] or with electromagnetic waves in the GHz range [97]. In applications of PC outside of fiber optics, the purpose is often to achieve spatial self-focussing [98], where e.g. an electromagnetic or acoustic wave is focussed back on its source after reflection in a phase conjugating mirror. In the context of lightwaves, the process of PC is referred to as OPC.

3.1.1 Mathematical description of phase conjugation

Here follows a short description of the phase conjugation operation. This is the optical signal processing operation that is performed both by the copier in a copier-PSA link as well as by the OPC devices in an OPC link. The process of PC can be described mathematically in either the time domain or in the frequency domain. In the time domain, phase conjugation is a complex conjugation of the electrical field in phasor notation which will be denoted

$$E(t) \overset{\hat{\mathrm{PC}}}{\Longrightarrow} E^*(t). \tag{3.1}$$

The PC process in frequency domain will then be the Fourier transform of both sides which is

$$\tilde{E}(\omega) \overset{\hat{\mathrm{PC}}}{\Longrightarrow} \tilde{E}^*(-\omega). \tag{3.2}$$

In Eq. (3.2) we see the reason why OPC sometimes is referred to as MSSI, since ω changes sign. The PC process in time and frequency domain is illustrated in Fig. 4.1. In time domain the signal is mirrored with respect to the real axis, flipping the sign of the imaginary part. In frequency domain,

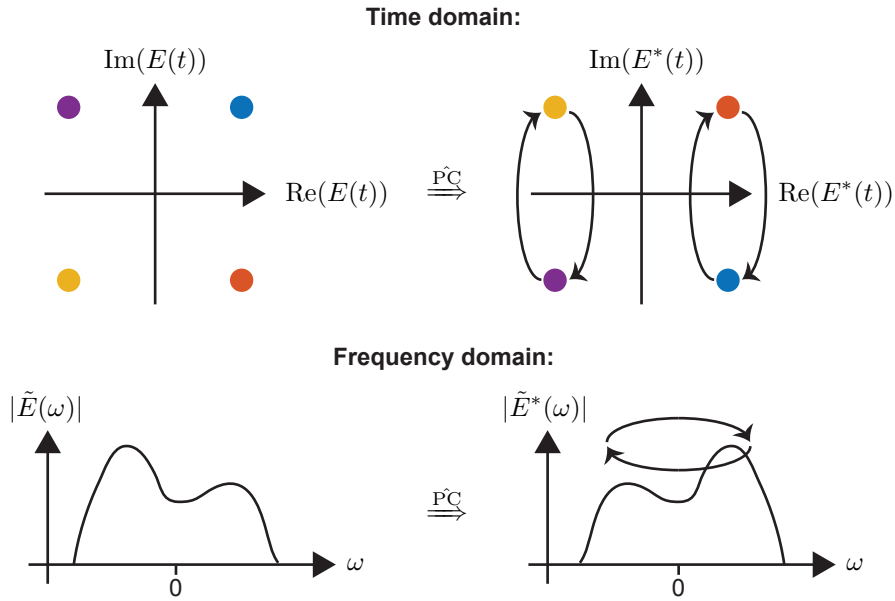

Figure 3.1: An illustration of PC of a QPSK constellation diagram in the time domain (top row) and PC of an arbitrarily shaped asymmetric spectrum in the frequency domain (bottom row).

the Fourier transform of the signal is inverted with respect to ω and complex conjugated. The inversion of the signal in the frequency domain provides an intuitive understanding of why it is possible to reverse the effects of β_2 by performing MSSI since the spectral components of the transmitted signal with higher group velocity will have a lower group velocity after OPC. With the same reasoning we also understand why the effects of odd orders of dispersion, e.g. β_3, cannot be reversed.

3.1.2 Methods for phase conjugation of light

There are several methods that can be used to phase-conjugate light or generate a phase-conjugated copy of a lightwave. The methods range from the use of nonlinear effects such as FWM [99] and stimulated Brillouin scattering (SBS) [100] to generation in digital domain [43, 101]. There are many different nonlinear media that can be used, ranging from e.g. semiconductor optical amplifiers [102] or periodically poled lithium niobate (PPLN) waveguides [94] to what we used in the appended papers which is highly nonlinear

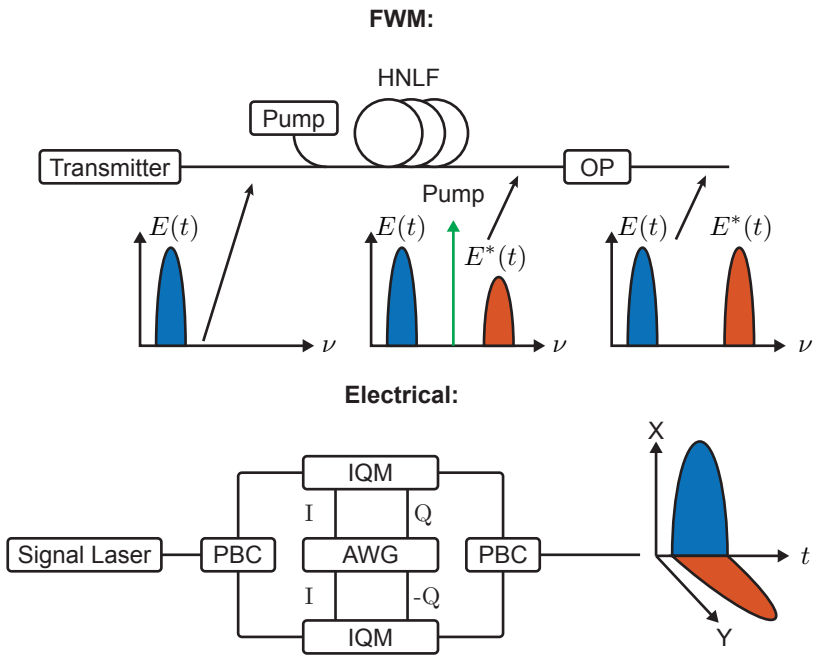

Figure 3.2: (top row) An illustration of generation of a phase-conjugated copy using FWM. The pump is filtered out in the optical processor (OP). (bottom row) Electrical generation of a phase-conjugated copy. For the electrical case it is assumed that no dispersion pre-compensation is applied. I and Q are the electrical driving signals for the in-phase and quadrature component to the IQ modulators. Polarization beam combiner/splitter (PBC), arbitrary waveform generator (AWG), IQ modulator (IQM)

fiber (HNLF) [103]. It is possible to generate a conjugated waveform in transmitter DSP which is then modulated on a continuous wave (CW) using a digital-to-analog converter (DAC)-driven IQ-modulator. In the following we will discuss in more detail the methods that were used in the appended papers and their strengths and weaknesses for different applications.

One common method to generate a phase-conjugated copy of a signal in fiber optics is through FWM between a signal wave and a high-power pump wave in a HNLF [104]. When using this method the phase-conjugated wave propagates in the same direction as the original wave and the carrier frequencies of the three waves fulfill $\omega_S + \omega_C = 2\omega_P$ where ω_S, ω_C and ω_P are the

frequencies of the signal wave, phase-conjugated wave and pump wave, respectively. An important property of the signal and phase-conjugated waves generated through FWM is that they are phase-locked. Phase-locked waves are a requirement if the waves are to be amplified by a PSA with stable gain. A drawback of this method is that the only way of applying dispersion pre-compensation on both the signal and phase-conjugated wave is all-optically using e.g. DCFs or FBGs, limiting the amount of dispersion pre-compensation that can realistically be applied. Another way of saying this is that the dispersion operator $\hat{D}$ and phase conjugation operator $\hat{PC}$ do not commute, i.e. changing the order that they are applied also changes the resulting output. This makes FWM-based methods incompatible with an antisymmetric dispersion map in a long-haul link, which is desired e.g. in a PCTW system, see section 4.2. An important advantage of FWM-based phase conjugation is that it makes it possible to generate phase-conjugated copies of e.g. WDM signals with large total bandwidth. This was done using a polarization-insensitive fiber-optic parametric amplifier in [105]. An illustration of the generation of a phase-conjugated copy or idler using FWM is illustrated on the top row in Fig. 3.2.

When discussing the generation of a phase-conjugated copy using FWM in a HNLF in this thesis, it will be assumed that there is one pump and one co-polarized signal present at the input to the HNLF. It is also possible to use dual-pump configurations where the two pumps are separated in frequency and on orthogonal polarization states as in [106, 107]. An in-depth discussion of such configurations is outside the scope of this thesis.

Other nonlinear effects such as e.g. SBS and SRS can also be used to perform phase conjugation [108, Chapter 7]. Such methods are often used in other fields than fiber optics but can not be considered as practical in the context of fiber optical communication with the purpose of phase conjugating a signal at high symbol rate. These methods will not be discussed at depth in this thesis.

A third method of generating a phase-conjugated wave is the one recently demonstrated in [43] where the signal and phase-conjugated waves were generated by modulating CW carriers with IQ-modulators driven by software-controlled DACs or an arbitrary waveform generator (AWG). This method is illustrated on the bottom row in Fig. 3.2. The benefit of this method is that it opens up the possibility to simultaneously apply dispersion pre-compensation for thousands of kilometers through transmitter side electronic dispersion compensation (EDC). The large amount of dispersion pre-compensation is needed in order to achieve an antisymmetric dispersion map over a long link which is required to optimize the mitigation of nonlinear distortion in PCTW systems.

This approach has its drawbacks as well, normally the peak-to-average power ratio of the signal will increase when dispersion pre-compensation is

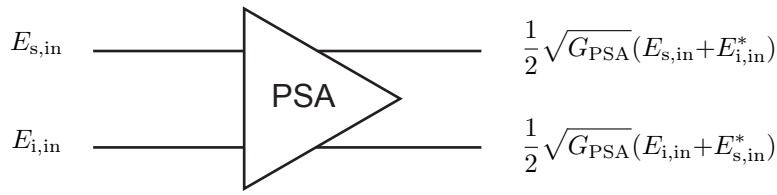

Figure 3.3: Illustration of the two-mode PSA transfer function according to the matrix definition in a high gain regime.

applied. Generating electrical drive signals with a high peak-to-average power ratio requires a large effective number of bits (ENOB) in the DAC in order to have good signal fidelity. It is worth to note that there are scenarios when this might not be true, e.g. if the signal has non-uniform statistics. Software-defined dispersion pre-compensation will also require a longer transmitter memory [16] increasing cost and power consumption. Another potential drawback of generation of a phase-conjugated wave in a software-defined transmitter is that the waves are not necessarily phase-locked. If e.g. two waves at different wavelengths are required to be phase-locked this can be solved by modulating different lines of e.g. an electro-optic [109], parametric [110] or microresonator-based [111] comb.

OPC can also be performed inline by performing coherent detection of the signal followed by inversion of the sign of the complex part of the signal and then re-modulating the phase-conjugated signal on a new carrier using an IQ-modulator. This was experimentally demonstrated in [101] and also later investigated in [112]. An advantage of this method is that it allows for free control of the signal wavelength after OPC by tuning the CW laser used in the OPC device. A downside of electro-optical OPC is that the bandwidth of the phase conjugation is limited by the bandwidth of the electrical components, i.e. photodetectors, electrical amplifiers and IQ-modulators making it challenging to perform OPC on several WDM channels with a single device.

3.2 Two-mode phase-sensitive amplifiers

The most basic definition of a phase-sensitive amplifier (PSA) is that it is an amplifier where the gain is dependent on the phases of one or more incoming waves. When we talk about PSAs in this thesis we mean fiber-optic parametric amplifiers (FOPAs) [113] that transfer energy from a high-power pump wave to

a signal/idler pair through FWM. This is done by inserting phase-locked signal and idler waves together with a high-power pump into a HNLF. It is important to note that there are many ways of implementing PSAs. Such amplifiers have also been demonstrated in other nonlinear media, e.g. PPLN [114] or silicon waveguides [115, 116]. In this thesis it will be assumed that the nonlinear medium is a HNLF.

In this thesis, only two-mode PSAs will be discussed, two-mode meaning that the signal and idler are located at two different wavelengths with the pump centered between them. There are other variants of PSAs [59], e.g. one-mode with signal and idler at the same frequency and four-mode with two pump waves and two signal-idler pairs. One-mode PSAs can be used to perform phase- and amplitude regeneration. By regenerating the phase of a signal it is also possible e.g. to mitigate nonlinear phase noise [117] due to the Kerr effect. Studies of such phase and amplitude regeneration can be found in e.g. [118–120]. A study of soliton propagation in a PSA link was presented in [121]. Not much work has been done on the performance in a nonlinear transmission regime of systems utilizing four-mode PSAs. The study of one-mode and four-mode PSAs is outside the scope of this thesis.

In two-mode copier-PSA links, a phase-locked idler wave at a different wavelength than the signal is generated through FWM at the transmitter side by inserting the signal together with a high power pump into a HNLF, this device is often called a copier. Both the signal, idler and pump are then propagated in the link. The PSA itself is very similar to the copier, also consisting of a HNLF, the difference being that both the signal and the phase-locked idler are inserted into the HNLF together with the pump which is what gives the PSA its unique properties.

In the context of optical signal processing, an interesting property of two-mode PSAs is that they they perform coherent superposition of the signal and idler waves, as a consequence of this, PSAs have a 0 dB quantum-limited NF [49]. That PSAs can mitigate nonlinear distortion due to the Kerr effect also comes from the fact that they perform coherent superposition. Coherent superposition is the simultaneous phase conjugation and addition of the signal field E_s and the idler field E_i according to [122]

$$\begin{pmatrix} E_{\mathrm{s,out}}(t) \\ E^*_{\mathrm{i,out}}(t) \end{pmatrix} = \begin{pmatrix} \mu & \nu \\ \nu* & \mu* \end{pmatrix} \begin{pmatrix} E_{\mathrm{s,in}}(t) \\ E^*_{\mathrm{i,in}}(t) \end{pmatrix}. \tag{3.3}$$

where the complex variables μ and ν satisfy

$$|\mu|^2 - |\nu|^2 = 1. \tag{3.4}$$

Assuming that the input signal and idler fields fulfill $E_\mathrm{i} = E^*_\mathrm{s}$ the maximum achieveble phase-sensitive gain becomes $G_\mathrm{PSA} = |\mu + \nu|^2$. The full expressions

for μ and ν can be found in [122] and will not be included here. In short, μ and ν depend on pump phase and power, dispersive and nonlinear properties of the HNLF and the length of the HNLF.

It is important to note that the way coherent superposition is used later in the derivation of PSA nonlinearity mitigation in section 4.4 relies on a high PSA gain. In that derivation it is assumed that $\mu \approx \nu$ which can only be true if $(|\mu| + |\nu|)^2 \gg 1$. An illustration of the PSA transfer function in a high gain regime is shown in Fig. 3.3. In the following, the focus will be on the coherent superposition property of PSAs since that is the property which has a big impact on the performance in a nonlinear transmission regime. Since the focus in this thesis is the properties of nonlinear distortion mitigation in PSAs, not much attention will be focussed on the advantageous NF of PSAs.

Chapter 4

All-optical nonlinearity mitigation

There are several different ways that phase conjugation can be used to mitigate nonlinear distortion due to the Kerr effect [123]. The method which was proposed first was OPC or MSSI in 1983 [26]. More recently, mitigation of nonlinear distortion using PCTW [43], CDR [Paper A] and the copier-PSA scheme [48], [Papers B-F] has been proposed. These three methods transmit a conjugated copy alongside the signal in different ways, mitigating nonlinear distortion at the expense of reduced SE. In this chapter we will first give a broad overview of the different methods followed by a more in-depth analysis of each separately. All of the methods which will be covered are illustrated in a simplified manner in Figs. 4.1 and 4.2. The first method illustrated in Fig. 4.1 is MSSI where the signal is first propagated over $N_{span}/2$ fiber spans, where N_{span} is the total number of spans. At the center point of the link, the signal is phase conjugated leading to reversal of nonlinear distortion in the second half of the link. Also shown in that figure is the approach to place several inline OPC devices, more on this in section 4.1. In Fig. 4.2 we illustrate the methods that make use of a phase-conjugated copy alongside the signal. The first such method is PCTW where a phase-conjugated copy of the signal is transmitted on the orthogonal polarization. Coherent superposition is then performed in receiver DSP leading to mitigation of nonlinear distortion due to the nonlinear distortion on the signal and conjugate wave being reflected with regard to the origin. The second method is CDR, where the conjugated copy is transmitted in different time slots than the signal followed by coherent superposition of the the two pulse trains in receiver DSP. The last method is mitigation of nonlinear distortion using non-degenerate two-mode PSAs. In this case, a phase-conjugated copy of the signal wave is transmitted on a separate wavelength and the coherent superposition operation is performed

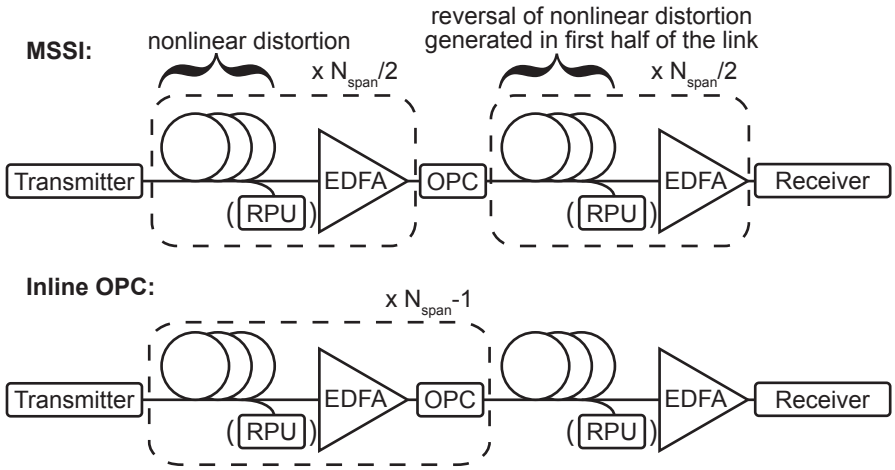

Figure 4.1: A simplified illustration of serial phase conjugation techniques: Mid-span spectral inversion (MSSI) (top row) and inline optical phase conjugation (OPC) (bottom row). Both cases are shown with optional backward pumped distributed Raman amplification (DRA).

all-optically in each inline PSA. In the following sections all of these methods will be discussed.

4.1 Optical phase conjugation

Optical phase conjugation for the purpose of mitigating nonlinear distortion due to the Kerr effect was first suggested by Fisher et al. in [26]. In that paper it was shown with a theoretical and numerical analysis that the combined effect of GVD and SPM on a pulse propagating in a dispersive nonlinear medium, e.g. an optical fiber, could be reversed by performing optical phase conjugation on the pulse followed by retraversal of the medium. In order to understand this phenomenon we look at the propagation equation for the waveform before and after OPC. The propagation equation for a single polarization signal, i.e. setting $E_{\mathrm{Y}} = 0$ in Eq. (2.9) is

$$\frac{\partial E_{\mathrm{X}}}{\partial z} = -\frac{i\beta_2}{2}\frac{\partial^2 E_{\mathrm{X}}}{\partial t^2} + \frac{g(z) - \alpha(z)}{2}E_{\mathrm{X}} + i\gamma|E_{\mathrm{X}}|^2 E_{\mathrm{X}}. \tag{4.1}$$

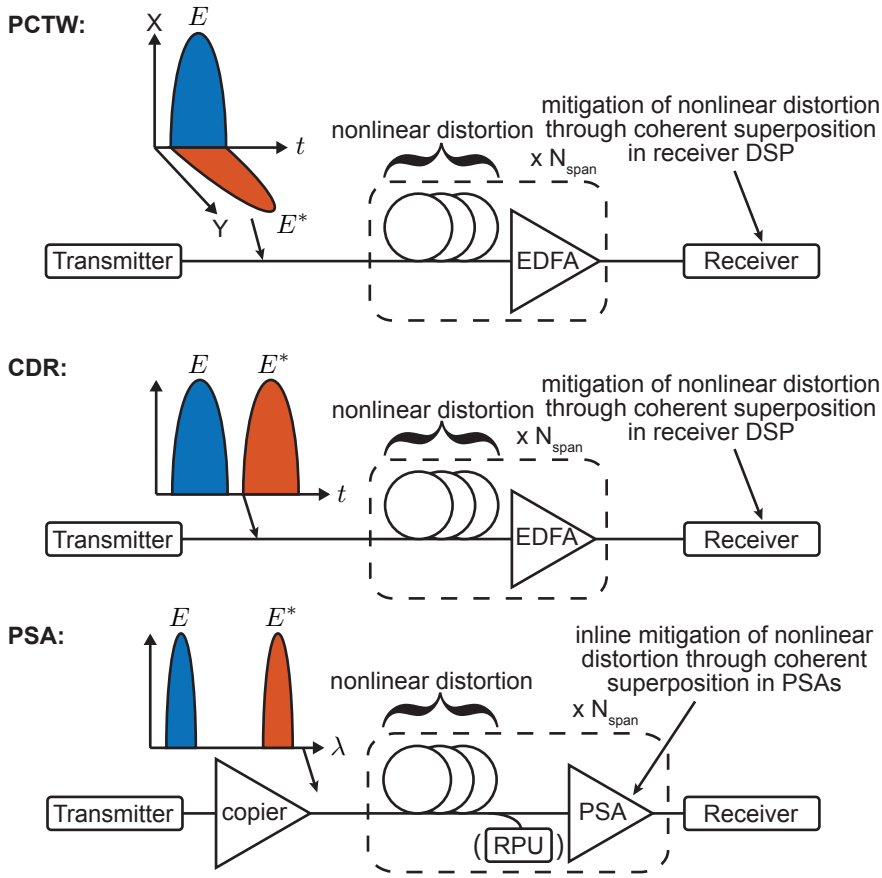

Figure 4.2: Simplified illustrations of nonlinearity mitigation methods using a phase-conjugated copy. The techniques are phase-conjugated twin waves (PCTW) (top row), conjugate data repetition (CDR) (middle row, investigated in [Paper A]), the two mode copier-PSA scheme (bottom row) with optional distributed Raman amplification (DRA), investigated in [Papers B-F].

By complex conjugating the propagation equation we get the propagation equation for the conjugated waveform

$$\frac{\partial E_{\mathrm{X}}^*}{\partial z} = \frac{i\beta_2}{2}\frac{\partial^2 E_{\mathrm{X}}^*}{\partial t^2} + \frac{g(z)-\alpha(z)}{2}E_{\mathrm{X}}^* - i\gamma|E_{\mathrm{X}}^*|^2 E_{\mathrm{X}}^*. \tag{4.2}$$

We see that the signs of the GVD and SPM terms are changed, meaning that the effects of both GVD and SPM can be reversed.

The term containing α is real-valued and thus does not change sign. In order for GVD and SPM to be reversed perfectly, we need a transparent fiber with $g(z)-\alpha(z) = 0$ or alternatively a power map which is symmetrical around the point where the OPC is performed. In practice we cannot have lossless fibers, however it is possible to have a power map with a higher degree of symmetry around the OPC point by means of e.g. distributed Raman amplification. In recent years there has been a renewed interest in OPC, to a large extent sparked by investigations of Raman-amplified OPC systems [124, 125]. In [95], the performance of long-haul systems employing different Raman amplification schemes in conjunction with mid-link OPC was studied numerically. The results from a field trial of a real link employing MSSI was presented in [126]. In recent years, multi-span links employing both distributed Raman amplification and OPC have been demonstrated experimentally [30, 31]. A detailed numerical study of different Raman amplifier configurations in OPC systems was performed in [127]. A RFL-based DRA scheme with FBG reflectors at both ends of each span together with second-order Raman pumps was demonstrated in an OPC system in [128]. There are also other ways to use OPC for nonlinearity mitigation, in e.g. [129], OPC was used to create a pre-distorted signal with improved performance in the nonlinear regime.

Another recent area of research is systems that perform the OPC operation several times along the transmission path [28]. In [29] it was shown with a semi-analytic approach that by using $\mathrm{N_{OPC}}$ phase conjugators in the transmission path, the SNR can be improved compared to a system performing ideal DBP by

$$\Delta\mathrm{SNR} = \sqrt{\mathrm{N_{OPC}} + 1}, \tag{4.3}$$

which becomes a significant increase with many inline OPC devices. In a numerically modelled 9,600 km link with 119 inline OPC devices, this was shown to improve the SNR compared to a system employing ideal DBP by approximately 10 dB [29] due to the suppression of nonlinear signal-noise interaction. The approach of using several inline OPC devices in many ways resemble the approach of using inline PSAs which will be covered in section 4.4. One important difference compared to a system employing inline PSAs is that a system employing multiple inline OPC devices does not require a 50 % reduction in SE [130]. However, this is sometimes still the case since in many experimental implementations the phase conjugation also shifts the frequency of the signal so that the signal occupies different wavelengths before and after OPC.

An interesting question regarding links employing all-optical nonlinearity mitigation is the impact of polarization mode dispersion (PMD). One can intuitively understand that PMD will disrupt the symmetry conditions regarding the accumulated dispersion. This was investigated in [131] where it was found that PMD can be an important performance limiting factor for links employing several inline OPC devices. It was also found that one way of reducing

the negative impact of PMD is to increase the number of OPC devices. This is quite different from the approaches one could use to reduce the impact of PMD in links employing digital nonlinearity compensation, e.g. DBP. In this case one approach is to estimate the PMD transfer function and then take the PMD into account when back-propagating the field in the digital domain [38]. To the best of my knowledge, the impact of PMD in copier-PSA links has not been investigated and any such study lies outside the scope of this thesis.

4.2 Phase-conjugated twin waves

The concept of PCTW was introduced by Liu et al. in 2013 [43] and is illustrated in a simplified manner on the top row in Fig. 4.2. In [43] they used a frequency domain perturbation analysis to show that the nonlinear distortion on a signal and its conjugate copy transmitted on the orthogonal polarization, are reflected around the origin in the complex plane, assuming a symmetric power map and an antisymmetric dispersion map. The conclusion from the analysis was also confirmed experimentally in a recirculating loop experiment. In that experiment, the antisymmetric dispersion map was achieved by applying EDC in transmitter and receiver DSP. Coherent superposition was performed in receiver DSP, leading to the cancellation of nonlinear distortion to first order. An antisymmetric dispersion map has also been shown to reduce the complexity of perturbation-based nonlinearity pre-compensation [78]. The reason for this is that an antisymmetric dispersion map effectively reduces the memory length of the fiber-optic channel meaning that fewer symbols have to be taken into account when calculating the generated nonlinear perturbation. In the context of PCTW, coherent superposition is the addition of the two fields E_{X} and E_{Y} according to

$$E_{\mathrm{CS}} = E_{\mathrm{X}} + E_{\mathrm{Y}}^{*}, \tag{4.4}$$

where E_{X} is the signal on the X-polarization and E_{Y} is the conjugated copy of the signal transmitted on the Y-polarization. The theory of PCTW was then generalized in [44] to include other signalling dimensions for the conjugated copy such as time [Paper A], SDM modes [132] or wavelength [47] for the conjugate copy. In [44], the concept was also extended to include phase conjugation of an entire WDM spectrum leading to mitigation of inter-channel nonlinear effects as well. This was demonstrated in [105] in a system with inline dispersion compensation. It is challenging to simultaneously phase conjugate and dispersion pre-compensate an entire WDM spectrum. The approach of the experimental demonstration in [43], with dispersion pre-compensation applied in the electrical domain in transmitter DSP, requires that all channels are modulated simultaneously. This would require a very high transmitter bandwidth, effectively covering the whole WDM spectrum bandwidth. Such a transmitter

can e.g. be built by using several synchronized software-defined transmitters modulating different lines of an optical comb. This was demonstrated with the purpose of doing transmitter-side pre-compensation for both intra-channel and inter-channel nonlinear effects in [35].

When considering the mitigation of nonlinear distortion in PCTW systems it is important to note that the theory in [43] is only valid to first order. The derivation does not take signal-noise interaction or higher-order signal-signal interaction into account. This is an important difference compared to OPC since the theoretical explanation for the mitigation of nonlinear distortion in OPC systems show that also higher-order nonlinear distortion can be reversed. However, this does not mean that PCTW does not mitigate higher-order nonlinear effects but that it is unknown what happens with higher-order nonlinear effects.

The two remaining methods for mitigation of nonlinear effects, CDR and PSAs can be formulated in the generalized sense as PCTW systems [44]. CDR can be formulated as a certain implementation of generalized PCTW in time domain while two-mode PSA links can be formulated as generalized PCTW in frequency domain. For a multi-span PSA system it is important to point out that the coherent superposition operation is performed not once in receiver DSP like in a PCTW system but several times all-optically in each of the inline PSAs.

An interesting property of a PCTW signal with the phase-conjugated wave transmitted on the orthogonal polarization is that it, under certain polarization rotations, is a PM-pulse-amplitude modulation (PAM) signal. This is the same thing as saying that the signal is real-valued under certain polarization rotations. This can be seen by considering the polarization rotation by a matrix

$$\frac{1}{\sqrt{2}}\begin{pmatrix}1 & 1\\ -i & i\end{pmatrix}\begin{pmatrix}E_{\mathrm{X}}\\ E_{\mathrm{Y}}\end{pmatrix}=\frac{1}{\sqrt{2}}\begin{pmatrix}1 & 1\\ -i & i\end{pmatrix}\begin{pmatrix}E_{\mathrm{X}}\\ E_{\mathrm{X}}^{*}\end{pmatrix}=\sqrt{2}\begin{pmatrix}\mathrm{Re}(E_{\mathrm{X}})\\ \mathrm{Im}(E_{\mathrm{X}})\end{pmatrix}, \tag{4.5}$$

where the field after the rotation is real valued in both polarizations. Assuming that the signal in E_{X} is 4^M-ary QAM, the real valued signals after the polarization rotation will be 2^M-ary PAM. Under this polarization rotation, the nonlinear distortion, which is seen as reflected with regard to the origin on the two polarizations in the PCTW picture, becomes purely imaginary and thus orthogonal to the infomation-carrying quadratures [44].

4.3 Conjugate data repetition

The concept of conjugate data repetition (CDR) [Paper A] can be formulated as PCTW in a generalized form [44] where the conjugated copy is transmitted

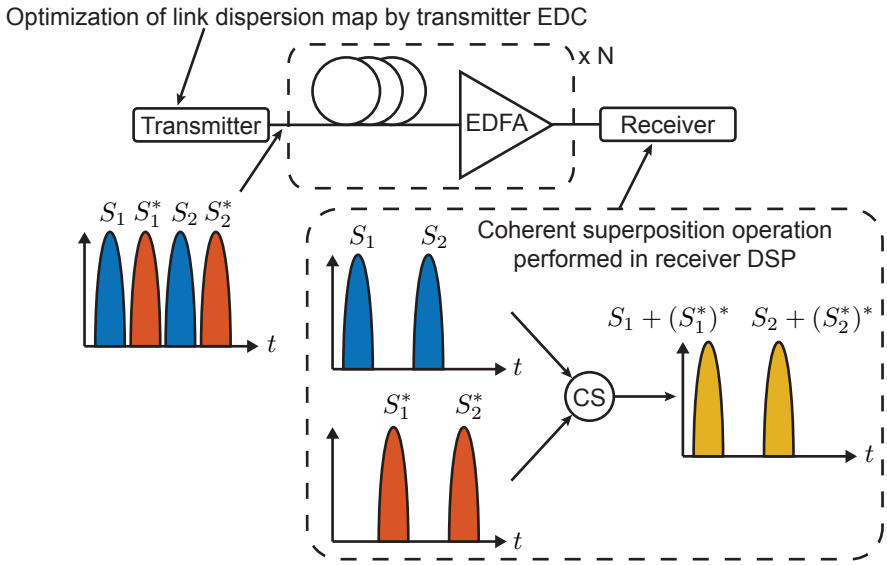

Figure 4.3: Schematic of the CDR link that was investigated in [Paper A]. A conjugated copy of each symbol is transmitted in the consecutive symbol slot. In receiver DSP, the signal pulse train is coherently superposed with the conjugate copy pulse train and part of the nonlinear distortion generated during propagation is mitigated.

in different time slots instead of on the orthogonal polarization. The concept is illustrated in Fig. 4.3. In transmitter DSP, one signal pulse train modulated with e.g. QPSK and one phase-conjugated copy of the signal pulse train is generated. The two pulse trains are then interleaved in time and pre-EDC giving an antisymmetric link dispersion map is applied. In receiver DSP, one of the pulse trains is delayed one symbol, phase-conjugated and then the two pulse trains are added. The idea to repeat conjugated data has also been investigated for interference cancellation in wireless links in [133]. For a PM-CDR signal, independent CDR pulse trains are transmitted on orthogonal polarization states. This concept was investigated numerically and with a time domain perturbation analysis in [Paper A]. With the time domain perturbation analysis it was shown that the nonlinear distortion on a train of CDR Gaussian pulses can be mitigated to a large extent through coherent superposition of the signal and conjugate pulse train in receiver DSP. This is in contrast to the case of PCTW, where the mitigation of nonlinear distortion is complete in a first-order perturbation analysis [43]. Despite this, it was found in the numerical simulations that CDR has comparable performance to conventional

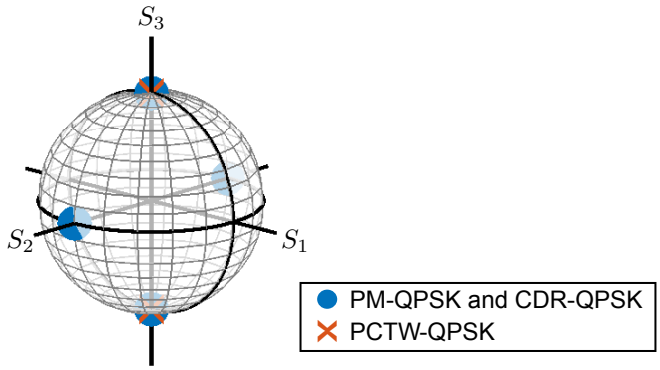

Figure 4.4: The points occupied on the Poincare sphere by PM-QPSK, CDR-QPSK and PCTW-QPSK.

PCTW.

An important difference when comparing CDR to PCTW is that the signal and its phase-conjugated copy occupy the same polarization. This could lead to an advantage when accounting for polarization dependent loss (PDL) and PMD but a thorough investigation of penalties due to these effects is beyond the scope of this thesis. Another argument for the use of CDR is that the conventional constant modulus algorithm (CMA) often used in coherent PM-QPSK systems will work for CDR-QPSK but not for PCTW-QPSK. This could lead to easier implementation in existing PM-QPSK systems since the same equalizer can be used for both PM-QPSK and CDR-QPSK. The reason behind this is the number of polarization states that the signal occupies, PM-QPSK and CDR-QPSK occupy four points on the Poincare sphere while PCTW-QPSK occupies only two. In order to show this we calculate the Stokes parameters [134]

$$\begin{pmatrix} S_0 \\ S_1 \\ S_2 \\ S_3 \end{pmatrix} = \begin{pmatrix} |E_\mathrm{X}|^2 + |E_\mathrm{Y}|^2 \\ |E_\mathrm{X}|^2 - |E_\mathrm{Y}|^2 \\ 2\,\mathrm{Re}(E_\mathrm{X} E_\mathrm{Y}^*) \\ 2\,\mathrm{Im}(E_\mathrm{X} E_\mathrm{Y}^*) \end{pmatrix}, \tag{4.6}$$

for CDR-QPSK and PCTW-QPSK signals. For CDR-QPSK we find all symbols by considering all permutations of $E_\mathrm{X} = (\pm 1 \pm i)/\sqrt{2}$ and $E_\mathrm{Y} = (\pm 1 \pm i)/\sqrt{2}$, this is the same symbol set as for PM-QPSK. For a CDR-QPSK signal,

this gives us the Stokes parameters

$$\begin{pmatrix} S_{0,\mathrm{CDR}} \\ S_{1,\mathrm{CDR}} \\ S_{2,\mathrm{CDR}} \\ S_{3,\mathrm{CDR}} \end{pmatrix} = \begin{pmatrix} 1 \\ 0 \\ 0, \pm 1 \\ 0, \pm 1 \end{pmatrix}. \tag{4.7}$$

For PCTW-QPSK we have, $E_{\mathrm{X}} = (\pm 1 \pm i)/\sqrt{2}$ and $E_{\mathrm{Y}} = E_{\mathrm{X}}^*$ which gives us the Stokes parameters

$$\begin{pmatrix} S_{0,\mathrm{PCTW}} \\ S_{1,\mathrm{PCTW}} \\ S_{2,\mathrm{PCTW}} \\ S_{3,\mathrm{PCTW}} \end{pmatrix} = \begin{pmatrix} 1 \\ 0 \\ 0 \\ 0, \pm 1 \end{pmatrix}. \tag{4.8}$$

The points occupied on the Poincare sphere by the signal using the different schemes are illustrated in Fig. 4.4. The conventional CMA commonly used in coherent PM-QPSK systems has a cost function which is designed for a signal occupying four polarization states and will not function properly if there are only two. It is however possible to alter the cost function of the CMA so that it converges with two polarization states instead of four [135].

In [Paper A] we presented theory and simulation results. Since then the concept of CDR or time-domain generalized PCTW has been investigated in an experiment as well. In [136] it was experimentally implemented in a comparison between different methods for nonlinearity mitigation in an 11-channel WDM 32 Gbaud 16-QAM link. The compared scenarios were uncompensated transmission, PCTW, CDR, DBP and cross-phase modulation (XPM) mitigation based on a recursive least-squares algorithm. The digital XPM mitigation scheme that they studied in that paper was introduced in [137] as a means of mitigating XPM distortion in digital domain with access to the field of only one WDM channel. It was found in that paper that the CDR and PCTW perform similarly. This is interesting since the simulations as well as the theoretical derivation in [Paper A] predicted slightly worse performance in the CDR case due to incomplete cancellation in the time domain perturbation analysis.

4.4 The copier-PSA scheme

The property that improves the performance of a PSA link in a nonlinear transmission regime is the fact that PSAs perform coherent superposition defined in Eq. 3.3. In the following, an explanation of why nonlinear distortion can be mitigated in a single-span PSA link, as depicted in Fig. 4.5 (with N = 1), will be provided. A frequency domain perturbation approach will be used, similar

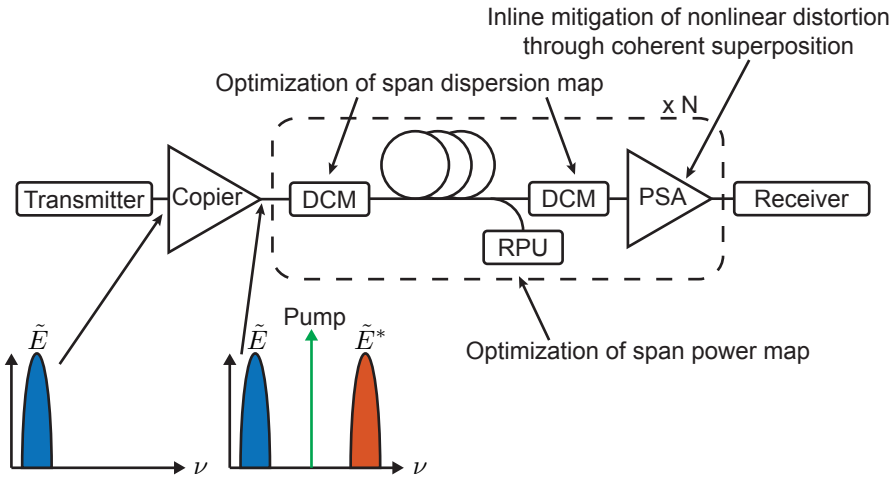

Figure 4.5: Schematic of a two-mode copier-PSA link. Dispersion compensating module (DCM), Raman pump unit (RPU).

to the analysis performed in [43] but instead of having the phase-conjugated copy propagating on the orthogonal polarization, the two waves will be considered to be propagating independently of each other since they are typically separated by approximately 10 nm in the kind of copier-PSA links studied in this thesis.

Now follows a derivation of the mitigation of nonlinear distortion in a single-span PSA link based on the perturbation analysis presented in section 2.6. The first step of the derivation is to calculate the nonlinear perturbation generated on the signal and idler waves. The transmitted signal and idler waves $u_{\mathrm{s}}^{(0)}$ and $u_{\mathrm{i}}^{(0)}$ satisfy the following relations

$$u_{\mathrm{i}}^{(0)}(t) = u_{\mathrm{s}}^{(0)*}(t) \text{ and } \tilde{u}_{\mathrm{i}}^{(0)}(\omega) = \tilde{u}_{\mathrm{s}}^{(0)*}(-\omega), \tag{4.9}$$

and by inserting these expressions into Eq. (2.27) we find the perturbation generated on the signal and idler waves after propagation over a fiber of length L to be

$$\tilde{u}_{\mathrm{s}}^{(1)}(L,\omega) = i\gamma P_0 L_{\mathrm{eff}} \int_{-\infty}^{\infty} \mathrm{d}\omega_1 \int_{-\infty}^{\infty} \mathrm{d}\omega_2 \eta(\omega_1,\omega_2) \times \tilde{u}_{\mathrm{s}}^{(0)}(\omega+\omega_1)\tilde{u}_{\mathrm{s}}^{(0)}(\omega+\omega_2)\tilde{u}_{\mathrm{s}}^{(0)*}(\omega+\omega_1+\omega_2), \tag{4.10}$$

and

$$\tilde{u}_{\mathrm{i}}^{(1)}(L,\omega) = i\gamma P_0 L_{\mathrm{eff}} \int_{-\infty}^{\infty} \mathrm{d}\omega_1 \int_{-\infty}^{\infty} \mathrm{d}\omega_2 \eta(\omega_1,\omega_2) \times \tilde{u}_{\mathrm{i}}^{(0)}(\omega+\omega_1)\tilde{u}_{\mathrm{i}}^{(0)}(\omega+\omega_2)\tilde{u}_{\mathrm{i}}^{(0)*}(\omega+\omega_1+\omega_2). \quad (4.11)$$

Next we assume an antisymmetric dispersion map and symmetric span power map such that

$$C(z) = -C(L-z) \text{ and } G(z) = G(L-z), \quad (4.12)$$

see section 2.6 for the definitions of $G(z)$ and $C(z)$. Under these assumptions, we see upon close inspection of Eq. (2.28) that $\eta(\omega_1,\omega_2)$ becomes real-valued, so that $\eta(\omega_1,\omega_2) = \eta^*(\omega_1,\omega_2)$. Using this together with the relationships in Eq. (4.9) we find that

$$\tilde{u}_{\mathrm{i}}^{(1)}(L,\omega) = -\tilde{u}_{\mathrm{s}}^{(1)*}(L,-\omega), \quad (4.13)$$

which is equivalent to

$$u_{\mathrm{i}}^{(1)}(L,t) = -u_{\mathrm{s}}^{(1)*}(L,t). \quad (4.14)$$

If we then perform the coherent superposition of the nonlinearly perturbed signal and idler fields according to Eq. (3.3) and use Eq. (4.14) we get

$$\begin{aligned} E_{\mathrm{s,out}} &= E_{\mathrm{s,in}}(L,t) + E_{\mathrm{i,in}}^*(L,t) \\ &= \sqrt{P_0}\exp\left(\frac{G(z)}{2}\right)\left[\tilde{u}_{\mathrm{s}}^{(0)}(t) + \tilde{u}_{\mathrm{s}}^{(1)}(L,t) + \tilde{u}_{\mathrm{i}}^{(0)*}(t) + \tilde{u}_{\mathrm{i}}^{(1)*}(L,t)\right] \\ &= \sqrt{P_0}\exp\left(\frac{G(z)}{2}\right)\left[2\tilde{u}_{\mathrm{s}}^{(0)}(t)\right], \end{aligned} \quad (4.15)$$

and we see that the nonlinear perturbation terms disappear to first order in the coherent superposition operation.

Several approximations and assumptions have been made to reach this conclusion. First, it is assumed that the signal and idler waves do not interact nonlinearly with each other during propagation. This is reasonable since they are assumed to be separated by approximately 10 nm and walk-off will limit the nonlinear interaction. Second, it is assumed that β_2 is the same at the signal and idler wavelength. In reality, the value of β_2 has a wavelength dependence and higher-order dispersion is ignored. Third, it is assumed that the power evolution during propagation $G(z)$ is identical for the signal and idler waves as well as symmetric. In reality, the attenuation is slightly wavelength dependent. Also, a perfectly symmetric power map can not be achieved in practice even with advanced DRA schemes. It is however possible to come close, in [67] a 80

km Raman amplified span was demonstrated with optical power excursions of only ±0.4 dB. Another important thing to point out is that this derivation is valid for a single-span link that uses one PSA before the receiver, performing coherent superposition only once. In a strict sense, the derivation is not valid for a multi-span PSA link with a PSA after each span. However, it is not unreasonable to approximate a multi-span PSA link as the concatenation of many single-span links, still this derivation will not tell us, e.g., what the optimal dispersion map in a multi-span PSA link is.

4.4.1 Inline dispersion compensation in PSA links

As discussed in the previous section and in [Papers B–F], optimization of the ratio between dispersion pre- and post-compensation in each span is important in order to have efficient nonlinearity mitigation in copier-PSA links. Even disregarding the properties of nonlinearity mitigation, full dispersion compensation of the signal and idler before the PSA is required to achieve phase-sensitive operation. An important consideration when discussing inline dispersion compensation in PSA links is that there is a trade-off between improving nonlinearity mitigation and reducing span losses. It could be that in terms of nonlinearity mitigation the optimum is, e.g. as was found for the PSA case in [Paper F], dispersion pre-compensation by 15 km. On the other hand, in terms of reducing the equivalent span NF, the optimum is to perform only dispersion pre-compensation. Dispersion pre-compensation can be performed after the amplifier where the optical power is high relative to before the amplifier causing a negligible span NF penalty. The losses from dispersion post-compensation will however translate directly to an increase in span NF since the post-compensation has to be done before the PSA.

In the appended papers we focused mainly on the understanding and optimization of nonlinearity mitigation in PSA links and did not consider e.g. the case where the dispersion post-compensation was set to zero. To study this trade-off in detail is beyond the scope of this thesis but the main considerations in the comparison would be the penalty induced by increased span losses due to dispersion post-compensation in relation to how much can be gained by nonlinearity mitigation. By looking at e.g. Fig. 2(a) in [Paper F] we see that the penalty in the nonlinear regime is very high and that the transmission reach is significantly reduced for the case with full dispersion pre-compensation. One can also note that the importance of the span dispersion map depends on e.g. symbol rate, number of WDM channels, modulation format etc. In some scenarios, the negative impact of a "bad" dispersion map could be large while in some scenarios it could be small depending on system parameters. Now follows a discussion on the two most commonly used techniques for inline dis-

persion compensation as well as important considerations in the context of PSA nonlinearity mitigation.

The first method for inline dispersion compensation that we will discuss is the use of dispersion compensating fiber (DCF) [8]. A DCF is an optical fiber where the fiber geometry as well as the refractive index of the different regions have been designed so that the dispersion profile of the fiber is inversed relative to that of the fiber it is designed to compensate. Normally the magnitude of the dispersion parameter is larger so that the DCF is much shorter than the SMF it is designed to compensate for. The dispersion compensation of modern DCFs can be very accurate and dispersion slope-matched to a certain SMF design with high precision [8]. In the context of PSA links there are however two important drawbacks of using DCF. The first one is that losses are generally higher compared to the FBG technique that will be discussed in the next paragraph. In PSA links the loss of the dispersion post-compensation is crucial and it is desireable to make it as low as possible. Second, DCF has a relatively high fiber nonlinearity coefficient and precautions have to be taken when designing links so that the impact of this is as low as possible. This could become difficult in e.g. a hybrid PSA-DRA link since the optical power levels can be high also after the transmission span. It could also become a larger problem in a link with highly efficient all-optical nonlinearity mitigation since the optical launch powers will be high.

A second common technique for inline dispersion compensation is the use of fiber Bragg grating (FBG)-based dispersion compensating modules (DCMs). A FBG is a short piece of fiber where a refractive index grating has been inscribed using laser light [9]. By designing a chirped grating it is possible to achieve a FBG transfer function which compensates for chromatic dispersion [138]. In the experiments presented in [Paper E] and [Paper F] we used DCMs based on channelized FBG technology [139]. The main reason for using such DCMs in those experiments was that we wanted tunability of the dispersion pre- and post-compensation to allow for an experimental optimization of the span dispersion map. Tunability can be achieved directly by thermal control of a FBG [140, 141] or with FBGs in a Gires-Tournois interferometer configuration [142]. Dynamic tunability can not be achieved using DCF-based DCMs which provide a fixed amount of dispersion compensation. An important advantage of using FBGs for dispersion compensation is that the insertion loss can be made lower for large amounts of dispersion compensation. It is also worth to note that fiber nonlinearities in FBGs are negligible since the fiber itself is very short. One of the major drawbacks of using this technology is the group delay ripple (GDR) due to nonidealities in the fabrication of the grating [143, 144]. The GDR is a random fluctuation in the phase response of the FBG on top of the desired quadratic phase response to compensate for second-order dispersion. FBGs can be designed for continuous or channelized

Table 4.1: Comparison between DCF- and FBG-based dispersion compensation for PSA links in terms of excess loss, induced nonlinear phase shift (NLPS) and phase ripple. The specified excess loss is for a fully dispersion compensated 80 km span with 15 km dispersion pre-compensation optimized for nonlinearity mitigation as in the PSA case in [Paper F]. The induced nonlinear phase shift (NLPS) and loss for the DCF is estimated according to [8] assuming the low loss "LLDK" DCF. The data for the FBG column is taken from a data sheet for a typical commercially available DCMs [145]. Note that e.g. the loss values represent what should be possible in an ideal scenario with fixed DCMs. The values are not representative of the DCM losses in the appended experimental papers.

	DCF	FBG
Excess loss [dB]	3.9	3.0
NLPS [% of total NLPS induced by DCM]	25	≈0
Phase ripple std [Radians]	≈0	0.1

dispersion compensation.

Both the DCF and FBG technologies are mature and commonly used. Which technology that is chosen in e.g. a certain commercial system can depend on factors such as cost or requirements on excess loss. A comparison between DCF- and FBG-based DCMs is presented in Table 4.1 where a few important device parameters are compared. The values in the table are meant to be representative of typical devices and should be considered as giving a general picture more than a detailed specific picture. One can also note that the best technique for inline dispersion compensation in PSA links could be a combination of the the two technologies with e.g. a DCF for pre-compensation and a FBG for post-compensation. This could lead to lower overall losses since a DCF-based DCM solution can have lower insertion losses for low dispersion compensation levels. In the experiments presented in [Paper E] and [Paper F] we used FBG-based channelized DCMs since this enabled an experimental sweep of the span dispersion map. This choice led to the GDR and bandpass characteristics of the DCMs causing penalties.

In order to understand the impact of GDR on the nonlinearity mitigation properties of PSA links we start by expressing the transfer function of the phase ripple of the GDR as a Fourier series [146]

$$H(\Delta\omega) = \exp\left(i\sum_j \phi_j \cos\left(\frac{\Delta\omega}{p_j} + \theta_j\right)\right) \tag{4.16}$$

where ϕ_j is the amplitude of phase ripple frequency component j, p_j the period, and θ_j the phase of the ripple relative to the carrier frequency. The phase ripple from the pre-compensation DCM will affect the nonlinear perturbation generated in the transmission span and taking the phase ripple into account, Eq. 4.10 describing the perturbation on the signal or idler becomes

$$\tilde{u}_{\mathrm{s,i}}^{(1)}(L,\omega) = i\gamma P_0 L_{\mathrm{eff}} \int_{-\infty}^{\infty} \mathrm{d}\omega_1 \int_{-\infty}^{\infty} \mathrm{d}\omega_2 \eta(\omega_1,\omega_2) \times H_{\mathrm{s,i}}(\omega+\omega_1)\tilde{u}_{\mathrm{s,i}}^{(0)}(\omega+\omega_1)H_{\mathrm{s,i}}(\omega+\omega_2)\tilde{u}_{\mathrm{s,i}}^{(0)}(\omega+\omega_2)H_{\mathrm{s,i}}(\omega+\omega_1+\omega_1)\tilde{u}_{\mathrm{s,i}}^{(0)*}(\omega+\omega_1+\omega_2), \tag{4.17}$$

and Eq. 4.13 will no longer be fulfilled since the phase ripple of the DCM for the signal H_{s} is different that for the idler H_{i}. From this reasoning it is clear that the phase ripple of the FBG-based DCMs could have a negative impact on the efficiency of the PSA nonlinearity mitigation. It does not however tell us how large the impact will be. For that, one would have to resort to numerical simulations using e.g. the SSFM for each specific case.

By inserting a phase filter between the copier and PSA stage of a two-mode copier-PSA arrangement it is possible to achieve optical filtering. This happens since the phase relation between the spectral components of the signal, idler and pump wave transfer directly to gain or attenuation in the PSA [147]. The analysis of the effects of GDR in FBG-based DCMs placed between the copier and PSA in a copier-PSA link is very similar to the analysis provided in [147], at least when considering a linear transmission regime. Such PSA-based optical filters were experimentally demonstrated in [148]. Later this was also investigated for the purpose of add-drop filtering in a Raman-assisted PSA [149] with an improved extinction ratio by 7.8 dB due to Raman amplification in the PSA.

4.4.2 Dispersion and power map optimization

In the steps leading up to Eq. 4.13 in the derivation of PSA nonlinearity mitigation it was assumed that the span dispersion map was antisymmetric and the span power map symmetric according to Eq. 4.12. This leads us to believe that it is important to choose a proper span dispersion map given a span power map in order to mitigate nonlinear distortion efficiently in a PSA link. At this point it is however important to note that the derivation shows that under the assumptions made in Eq. 4.12, the nonlinear distortion cancels out. It does not prove an equivalence in the other direction, i.e. that this is the only choice of power and dispersion map that will lead to ideal cancellation in a perturbation sense. This is important since it could be possible to design a power and dispersion map pair that would give ideal cancellation of the

nonlinear distortion without e.g. the power map fulfilling the conditions of symmetry assumed in Eq. 4.12.

The optimization of the span dispersion map in a copier-PSA link was first investigated in [150]. In that paper it was shown that by optimizing the dispersion map in a single-span copier-PSA link, it was possible to improve the tolerance against nonlinear distortion leading to 3 dB higher launch power for a 1 dB Q-factor penalty. In [151], the optimum dispersion map was found for different span lengths as well as different fiber loss coefficients leading to different span power maps. In all of these papers the dispersion map optimization was performed numerically. It is of course desirable to perform this optimization experimentally, this is made possible by the FBG technology that was discussed in Section 4.4.1. In [Paper E] we performed this optimization experimentally for a long-haul copier-PSA link transmitting a 10 GBaud QPSK signal. An experimental dispersion map sweep was also performed in a copier-PSA link transmitting a 16-QAM signal in [152]. We also performed this experimental dispersion map optimization in a 28 GBaud QPSK PSA link combining DRA and PSAs in [Paper F]. In that paper we also compared the results from the dispersion map optimization with and without DRA and it was seen that in the PSA-DRA case that the optimum shifted close to what is predicted by the theoretical analysis in Eq. 4.12. In summary, what has been learned from these studies is that several factors affect the dispersion map optimization. For a given PSA link, the optimum dispersion map depends on e.g. symbol rate and even modulation format, something which can not be understood by the perturbation analysis from section 4.4. When discussing dispersion maps one can also point out that the accumulated dispersion on the signal and idler has to be compensated close to zero before each PSA in order to achieve phase-sensitive operation [153]. In all of the mentioned dispersion map optimizations the residual dispersion was set to zero.

An extension of the span dispersion map optimization was presented in [Paper D] to allow for different span dispersion maps in the first and second span of a two span PSA link. It was shown in simulations that the two-span optimum was different for a PIA link and a copier-PSA link. This point is important since it tells us that there are additional effects on top of the gains that can be had by e.g. allowing for residual dispersion in the link [154]. It can be argued that part of the improvement that was observed in that paper is due to decorrelation of the residual nonlinear distortion not being cancelled in the first and second span. It is however not clear at the moment if this decorrelation effect is the whole explanation or if e.g. the bandwidth of the nonlinearity mitigation is improved when performing this multi-span dispersion map optimization. A full explanation of this phenomenon is beyond the scope of this thesis.

It is also important to note that the brute force approach based on the

SSFM used to optimize the multi-span dispersion map in [Paper D] quickly becomes intractable for many spans since the computational time required increases approximately as $(D_{maps})^N$, where D_{maps} is the number of dispersion maps investigated per span and N is the number of spans the optimization is performed over.

We will now discuss one method that could improve the understanding of this phenomenon and reduce the computational complexity of the brute-force approach in the process. One way of analyzing the multi-span dispersion map optimization is to extend the perturbation analysis presented in Section 4.4 to account for propagation over several spans. In contrast to the analysis in Section 4.4 one should not assume a flat power map but instead assume a regular power map with realistic loss and solve the integrals numerically. The analysis would assume different dispersion maps in different spans and analyze the magnitude of the residual nonlinear perturbation after the whole link. Since we have not performed this analysis it is also important to point out that it is not guaranteed that such an analysis actually would provide a better understanding. If, e.g. it would turn out that the first-order perturbation analysis of a single span with a regular power map shows ideal cancellation it would be difficult to learn anything from this analysis.

For a lossy fiber span it is a good first guess that the point around which the span power map has the highest degree of symmetry is close to $L_{\text{eff}}/2$ which is quite close to what was found for the PSA case in e.g. [Paper F]. Note also that it is not clear exactly how to define a metric for the degree of power map symmetry which will predict system performance well. In [30] a metric was suggested for OPC links based on integration of the difference in the power map before and after the OPC device over the link length. One could perform a similar analysis for the PSA case and try to use the prediction of the point around which the span power map symmetry is highest in order to choose a suitable dispersion map.

In [Paper F] there was no effort made to equalize the DRA gain at the signal and idler wavelength. Since the DRA scheme used a single backward Raman pump the gain spectrum was not flat over the whole 8 nm separation of the signal and idler wave. A measurement of the DRA gain spectrum in the segmented span is shown in Fig. 4.6. We note that the difference in span net gain between the signal and idler wavelength is approximately 0.9 dB. This will introduce a different kind of power map asymmetry between the signal and idler wave which will lead to penalties in a similar manner to power asymmetry around the OPC device in a OPC link. The most straightforward way of improving the gain spectrum flatness would be to introduce a multi-pump DRA scheme [155]. At this moment it is not fully clear how large the penalties due to the tilt in the DRA gain spectrum are. A more detailed

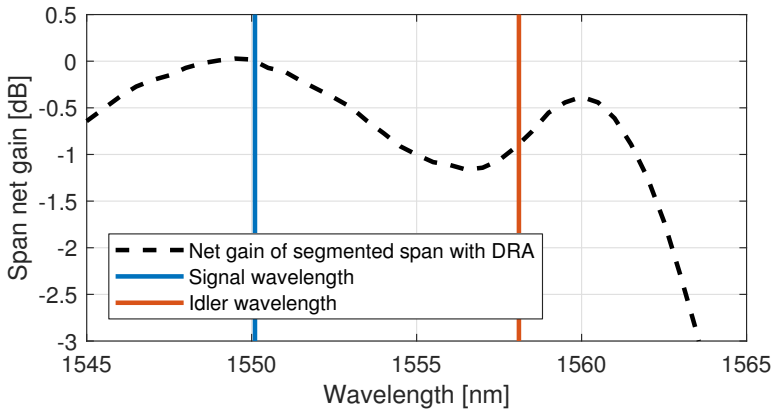

Figure 4.6: Measurement of the span net gain in the segmented span with DRA used in [Paper F]. Blue and red vertical lines represent the signal and idler wavelength. The span net gain has been normalized so that the gain at the signal wavelength is 0 dB in the same manner as in [Paper F].

investigation of this is beyond the scope of this thesis.

4.5 Comparing PSA and OPC links

Now follows a discussion on the comparison between different all-optical nonlinearity mitigation methods. This comparison will not focus on the comparison between all-optical and digital approaches like e.g. DBP. We will start with a discussion on the different methods and then present some simulation results comparing PSA, OPC and uncompensated links in a typical WDM transmission scenario.

An important aspect is the limitations imposed on the SE using all-optical nonlinearity compensation schemes compared to uncompensated transmission. In this regard, it is more beneficial to use OPC since that does not fundamentally require any reduction in SE. It is, however, important to point out that in many specific implementations of OPC, e.g. [27], SE is still reduced because of wavelength conversion. For the other methods, PCTW, CDR and the copier-PSA scheme, only half of the available signalling dimensions can be used to encode data on. One general conclusion from this is that if the goal is to achieve high SE, large performance gains in the nonlinear regime are required in order to motivate the transmission of a phase-conjugated copy. In this context it is also worth mentioning that there might be other technical reasons why it is not possible to utilize all of the available spectrum. In e.g.

the two-mode pump-degenerate copier-PSA scheme discussed in this thesis it is required to have guard bands around the pump reducing the utilization of the available spectrum. One can however point out that while we transmit the pump as well in the experiments of the appended papers, this is not fundamentally required. Another possibility is to completely regenerate the pump from the signal and idler waves using e.g. a χ^2 nonlinear medium as in [156]. There will be a further discussion on this in Chapter 6. Using other PSA implementations such as the vector copier-PSA scheme could also make it possible to utilize the spectrum more efficiently [110]. In [157], an OPC scheme using PPLN waveguides was implemented with essentially no loss in spectral efficiency. There could be limitations in the optical bandwidth of the optical signal processing devices but with development of suitable nonlinear media it should be possible to achieve sufficient optical bandwidth. In [158] a PSA was demonstrated with an optical bandwidth in excess of 170 nm.

When comparing the performance in the linear transmission regime, a system employing PSAs has an advantage because of the 0 dB quantum-limited NF. Using OPC, there is a quantum-limited NF of 3 dB associated with the inline amplification due to the nature of a phase-conjugating or phase-insensitive amplifier [58]. When discussing linear noise properties, it is important to note that for the simulated scenario studied in [Paper C] with a hybrid link using both distributed Raman amplification and PSAs, the 0 dB NF of the PSAs was not a significant advantage since the equivalent span NF was mostly dictated by the noise from the distributed Raman amplification. In the experimental demonstration of a PSA-DRA link in [Paper F] it was however the other way around, there were significant lumped losses before the PSA meaning that the equivalent span NF was mostly dictated by the PSA. In practice, the relationship between the noise added by the distributed Raman amplification and the inline optical signal processing devices will depend on e.g. the Raman pump scheme used, the span length and the magnitude of the lumped loss before the devices.

Now we will extend the discussion on the symmetry conditions in Eq. 4.12 and discuss some important differences regarding this when comparing copier-PSA links to OPC links, more on this comparison in the next section. To do this we must also take into account the relationship between the span power and dispersion map. In the preceding texts discussing PSA links it has been assumed that the starting point in the dispersion map optimization is a given span power map and then the dispersion map optimization is performed by sweeping the ratio between dispersion pre- and post-compensation. One could also turn this argument around and say that we start with a span dispersion map and then try to fulfill the span power map symmetry condition around the point with zero accumulated dispersion for the chosen dispersion map. In a PSA link, it is possible to choose the point around which span power

map symmetry is sought after by adjusting the span dispersion map. For the OPC case it was shown in [159] that it is theoretically possible to improve the fulfillment of power map symmetry conditions in a MSSI link with EDFAs by introducing a dispersion compensating element before or after the OPC device. In [160] it was shown in simulations that by inserting a DCM before the OPC device in a MSSI link it was possible to achieve a 3 dB Q-factor improvement. To the best of my knowledge this has not been studied in the case with multiple inline OPC devices and further studies of this could prove interesting. Another approach would be to optimize the position of the OPC device inside the transmission span. This is not realistic in practical systems, it is however possible to optimize the location of the OPC device in simulations and this was done in [161].

Another important issue is the required complexity of transmitters and receivers for the different schemes. In this regard, OPC- and PSA-systems are advantageous since they only require one hybrid receiver per channel. Neither OPC or PSA links require large amounts of transmitter and receiver EDC as is required in the PCTW or CDR case. In the case of OPC, EDC is not required at all ideally since the inline OPC devices also compensate for CD while for the case of PSAs it is required to use inline optical dispersion compensation.

An experimental comparison between the nonlinear distortion mitigation properties of mid-link OPC, PCTW, PSA and DBP systems was done in [162]. In that experiment it was found that the system performing coherent superposition in the digital domain performed best out of the four schemes. However, one can point out that e.g. the dispersion maps were not optimized in that experiment, leaving room for further optimization.

4.5.1 GMI comparison

The fact that only half of the available signalling dimensions are used in copier-PSA links makes it difficult to make direct comparison to e.g. OPC or uncompensated links. One way of handling this problem is to make comparisons in terms of mutual information (MI) [163] or generalized mutual information (GMI) [164]. The MI is a measure of the maximum achievable spectral efficiency given a certain modulation format and ideal FEC. A more realistic measure is the GMI where it is assumed that the FEC decoder is operating on the individual bits instead of e.g. symbols. In such a comparison, one would treat the copier-PSA scheme as a subset partitioned modulation format [165] selecting only the 4-D constellation points fulfilling $E_i = E_s^*$. If e.g. we want to compare a 16-QAM PSA link to an uncompensated 16-QAM link we would then estimate the GMI of the 4-D symbols directly [166]. In this way it is possible to account for the wider optical spectrum occupied in PSA links. This method can be used to make a comparison between a PSA link

and e.g. an uncompensated link to see if the 0 dB NF and nonlinearity mitigation properties provide sufficient benefits to make up for only using half of the available signalling dimensions. In [167] an experimental comparison between a PM-QPSK and a PCTW-QPSK link in terms of GMI was performed in this manner. It was found in that paper that the loss in SE using PCTW could not be motivated in terms of GMI at typical long-haul transmission distances. Worth to note here is that a GMI comparison makes sense if SE is an important metric. In some scenarios like e.g. long free-space optical links it could be that SE is not as important but other metrics like link budget and sensitivity are more important.

Now we will present simulation results from a GMI comparison between PSA, OPC and uncompensated long-haul links. An illustration of the simulated cases is shown in Fig. 4.7. The nonlinear Schrödinger equation (NLSE) governing the fiber propagation was solved using a SSFM solution of the Manakov equation [55]. The PSAs were modelled in a similar manner as in [Paper C] and the OPC devices was modelled as ideal phase conjugators. For the PSA case we chose a vector PSA [106, 110] implementation with signal and idler on orthogonal polarization states in order to make efficient use of available optical bandwidth. In both the OPC and PSA case there is one PSA or OPC device after each span. For each case we also simulate three amplifier configurations, no DRA, backward pumped DRA and ideal DRA. ASE noise due to DRA was added in each split-step and the step length was 12.5 m. The PSAs had a 1 dB NF and OPC devices and EDFAs had a 4 dB NF. In the PSA case, the span dispersion map was optimized for each case individually and the DCMs were considered ideal and lossless. The simulated systems transmitted 31 WDM channels at 49 GBaud on a 50 GHz spacing. The transmitted signals were modulated with root-raised-cosine (RRC)-shaped 16-QAM with a roll-off factor $\beta = 0.01$. All WDM channels were independently modulated with random data and 2^{14} symbols at a oversampling rate of 128. The fiber parameters were $L_{\text{span}} = 100$ km, $\alpha_s = 0.2$ [dB/km], $\alpha_{\text{Raman}} = 0.25$ [dB/km], D = 17 [ps/nm/km] and dispersion slope S = 0.09 [ps/nm^2/km]. The receiver consisted of simplified DSP with matched filtering followed by phase alignment and GMI estimation of the center channel.

The results from the simulations are shown in Fig. 4.8 where the GMI is shown as a function of the transmission distance for the different cases and amplifier configurations. A few things are important to note when looking at these results. First we note again that there is one PSA or OPC device placed after each span. This is not necessarily optimal, e.g. if the span power map shows a low degree of symmetry the nonlinearity mitigation will be inefficient and what is achieved is essentially moving to an inline dispersion compensated

system due to OPC devices or inline DCMs in the PSA case. This could lead to the optimum number of OPC devices being lower than one device per span [168]. We believe this to be the reason that e.g. the OPC EDFA and OPC Raman cases perform worse that the uncompensated EDFA and Raman cases. One could suspect then that the PSA and OPC EDFA cases would be penalized in a similar manner. Interestingly the PSA case performs better than the OPC EDFA case at distances above 60 spans. We believe this is due to the effects discussed in the end of section 4.4.2 where it was argued that the dispersion map optimization in PSA links chooses the point around which power map symmetry is sought after. If we instead focus on the comparison between PSA links and uncompensated links we see that it is not possible to achieve a higher GMI by addition of PSAs in any of the scenarios. If we compare e.g. the PSA case to the uncompensated EDFA case we see that the uncompensated EDFA link has a strictly higher GMI even at long distances.

It was predicted in [169] that the capacity of a two-mode copier-PSA link operating over a AWGN channel will be higher in a low SNR regime. In these simulations we can not find a regime where the GMI of the copier-PSA link is higher. One should point out two things regarding this, first that the simulated scenario is very different from a two-mode copier-PSA link operating over over an AWGN channel, still this comparison is interesting to make. Second that we propagated up to 200 spans, it is possible that the uncompensated EDFA curve and the PSA curve cross at even longer distances but we did not find it meaningful to propagate longer than 20 000 km. Another interesting comparison to make is that between the OPC link with ideal DRA and the PSA link with ideal DRA. Here one can compare e.g. the decrease in GMI at 200 spans. In the OPC case with ideal DRA the GMI has dropped from 3.92 to 3.83 representing a decrease by 2.3 %. In the PSA case with ideal DRA the GMI has dropped from 1.96 to 1.63 representing a decrease by 16.8 %. It is clearly seen that the GMI has been reduced more in the PSA case. Possible explanations for this could be phase-to-amplitude transfer in the coherent superposition operation of the PSAs [151] or as was discussed in section 4.4 that as far as we know, the mitigation of nonlinearities is only true in a perturbation sense.

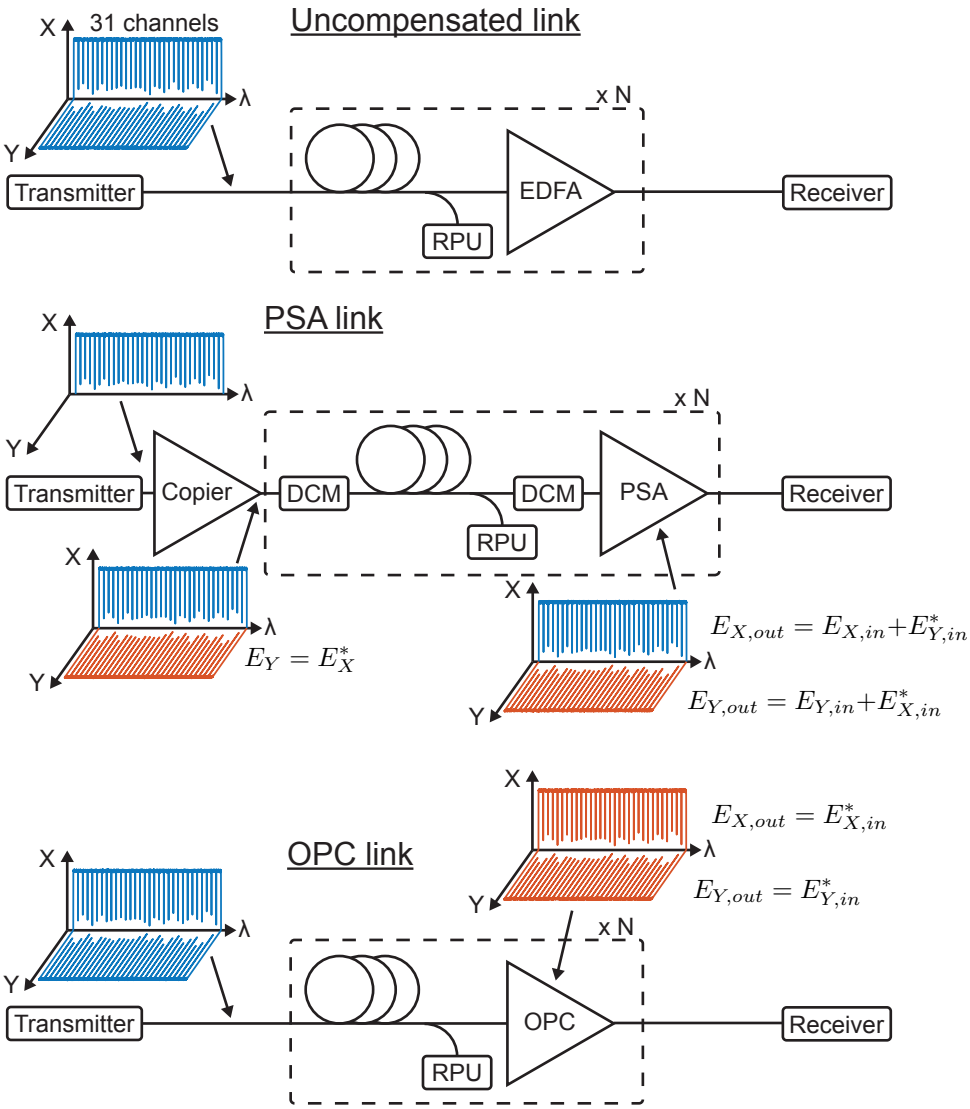

Figure 4.7: Illustration of the simulated setups in the GMI comparison. From top to bottom, the uncompensated link, PSA link and OPC link. Blue represents a signal and red its phase conjugate.

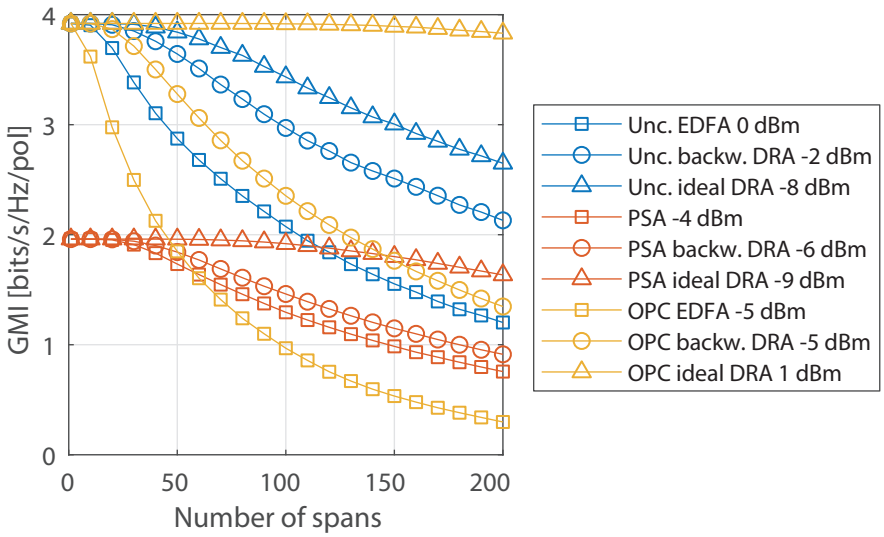

Figure 4.8: The GMI as a function of transmission distance for an uncompensated (blue), OPC (yellow) and PSA (red) link. Each case was simulated without DRA (squares), with backward pumped DRA (circles) and ideal DRA (triangles). All curves are at the optimum launch power and the launch power is stated for each case in the legend.

Chapter 5

Future outlook

In the following there will be a discussion on possible future directions for research in the areas of copier-PSA links, all-optical signal processing and nonlinearity mitigation.

5.1 Copier-PSA links operating in a low SNR regime

As mentioned in section 4.5.1 there are predictions that the capacity of a copier-PSA link would exceed that of a regular link with PIAs transmitting independent data on the signal and idler channel in a low SNR regime assuming an AWGN channel. To the best of my knowledge this has not been investigated or demonstrated experimentally. A study of this could focus either on transmission over e.g. a free space copier-PSA link or on transmission over fiber. The most straightforward way of investigating this is probably in a back-to-back or free space copier-PSA link so that the channel is closer to an AWGN channel. Even though it was seen in the simulations presented in section 4.5.1 that it was not possible to achieve a higher GMI in the studied scenario it should be stressed that this is no way a general conclusion. It could very well be possible to find scenarios with fiber transmission where the GMI of a copier-PSA link would be higher than that of a PIA link. Studies of the capacity of two-mode copier-PSA links can also be found in [169–171].

5.2 WDM copier-PSA links

One of the appealing properties of the copier-PSA scheme is WDM compatibility. Still no exhaustive studies have been performed on WDM copier-PSA

links. It was predicted in [Paper C] that the efficiency of the nonlinearity mitigation with a non-ideal span power map is reduced at high signal symbol rates. Exactly how this extends to a WDM scenario is unclear at the moment and further studies should investigate both the implementational difficulty of WDM copier-PSA links as well as improve the understanding of the impact of nonlinear distortion in such links. If it is found that the efficiency of the nonlinearity mitigation is reduced significantly in a WDM scenario it could be that the best thing to do is to optimize for linear regime performance by reducing dispersion post-compensation losses instead of optimizing the nonlinearity mitigation. A proper analysis would have to take both of these factors into account, something which has not been done up to this point.

5.3 Pump regeneration schemes

In the appended papers it was assumed that the pump was transmitted alongside the signal and idler wave and regenerated through injection locking. Assuming that the pump is CW there is no fundamental requirement that the pump has to be co-propagated with the signal and idler waves. One way of regenerating the pump is through sum-frequency generation in a $\chi^{(2)}$ material which was demonstrated in [156]. While this is one possibility it should also, at least in theory, be possible to have a free-running laser with a phase-locked loop (PLL) [172, 173] tuning the wavelength and phase to achieve phase-sensitive amplification of a signal and idler pair. In practice such a scheme for pump regeneration would probably be challenging to implement since the required precision in the wavelength tuning of the free-running laser is very high. This would also require ultra narrow linewidth lasers so that a PLL can continuously track the phase. A related study could be the impact of XPM from signal and idler onto the pump in a copier-PSA link since this is one of the issues that could be solved by not co-propagating the pump.

Chapter 6

Summary of Papers

[Paper A]

"Mitigation of nonlinearities using conjugate data repetition," *Optics Express*, vol. 23, no. 3, pp. 2392-2402, 2015.

In this paper, we investigate a scheme for mitigation of nonlinear fiber distortion based on the idea to send a phase-conjugated copy of each symbol in the consecutive symbol slot followed by coherent superposition of the two pulse trains in receiver DSP. The mitigation of nonlinear distortion is derived using a time domain perturbation analysis and we compare the efficiency of the nonlinearity mitigation to that of regular phase-conjugated twin waves in numerics. The results show that the performance in terms of transmission reach is comparable even though the perturbation analysis predict worse performance for CDR.

My contribution: I performed the theoretical and numerical modelling as well as the data analysis. I wrote the paper.

[Paper B]

"Comparison between coherent superposition in DSP and PSA for mitigation of nonlinearities in a single-span link," *Proceedings European Conference on Optical Communication (ECOC)*, Cannes, France, 2015, paper Mo.3.5.2.

An experimental comparison between the mitigation of nonlinear distortion in a single-span system performing coherent superposition all-optically in a PSA or in receiver DSP is presented in this paper. The performance in the nonlinear transmission regime is quantified with measurements of error vector magnitude (EVM) at different launch powers and optical signal-to-noise ratio (OSNR) penalty with noise loading. It is shown that the performance in the nonlinear regime is comparable with both approaches.

My contribution: I planned the experiment and performed the measurements with S. Olsson. I wrote the paper. I presented the paper at ECOC in Cannes, France in 2015.

[Paper C]

"Mitigation of nonlinear distortion in hybrid Raman/phase-sensitive amplifier links," *Optics Express*, vol. 24, no. 2, pp. 888-900, 2016.

A numerical investigation of the impact of the span power map in single-span and multi-span PSA links is presented in this paper. Three different link amplifier configurations are investigated, PSA only, PSA with first-order backward-pumped Raman amplification and PSA with ideal distributed Raman amplification. First, the optimum dispersion maps are found in the single-span scenario and the OSNR penalty as a function of launch power and NLPS is evaluated. Then, multi-span PSA links with the three different amplifier configurations are modelled using the optimum single-span dispersion maps. It is found that the transmission reach of a multi-span PSA link can be increased by as much as a factor of 8.1 by including ideal distributed Raman amplification and using the span dispersion map found to be optimal in the single-span scenario.

My contribution: I proposed the idea for the paper. I performed the numerical simulations and wrote the paper.

[Paper D]

"Dispersion management for nonlinearity mitigation in two-span 28 GBaud QPSK phase-sensitive amplifier links," *Optics Express*, vol. 25, no. 12, pp. 13163-13173, 2017

In this paper we presented a numerical and experimental study of the impact of the dispersion map in a 28 GBaud QPSK copier-PSA link. We proposed to optimize the dispersion map over two spans instead of one which had pre-

viously been investigated. It was shown that the optimum dispersion map is different in a PIA link and a PSA link, indicating that nonlinearity compensation through coherent superposition is a significant effect. The optimum 2-span dispersion map was then evaluated in an experiment exhibiting a 2 dB improvement in launch power tolerance compared to the optimum single-span dispersion map for the same EVM penalty.

My contribution: I assisted E. Astra in setting up and running the simulations. E. Astra, S. Olsson and I planned and built the experiment and performed the measurements.

[Paper E]

"Long-haul optical transmission links using low-noise phase-sensitive amplifiers," Manuscript under review.

In this paper we present results from a long-haul transmission experiment with inline PSAs. We transmit a 10 GBaud QPSK signal and observe benefits both in terms of the 0 dB quantum-limited NF as well as nonlinearity mitigation resulting in a transmission reach improvement by a factor of 5.6 at optimum launch powers when enabling phase-sensitive amplification. Remarkably this is higher that the four times improvement expected in the linear regime. The total accumulated nonlinear phase shift at optimum launch power was 6.17 rad.

My contribution: S. Olsson and I built the experiment and performed the measurements.

[Paper F]

"Phase-sensitive amplifier links with distributed Raman amplification," Manuscript to be submitted.

In this paper we present results from a long-haul transmission experiment utilizing both DRA and PSAs. DRA was included in an effort to improve the nonlinearity mitigation with a flatter power map. We present results from an experimental dispersion map optimization and the results match what is predicted by theory well. It was however not possible to demonstrate a higher total accumulated nonlinear phase shift with DRA even though the optimum launch power increased by 2 dB when enabling phase-sensitive amplification with DRA.

My contribution: I planned and built the experiment together with S. Ols-

son and E. Astra. I performed the measurements together with K. Vijayan and B. Foo. I wrote the paper.

References

[1] K. Kao and G. A. Hockham, "Dielectric-fibre surface waveguides for optical frequencies," in *Proceedings of the Institution of Electrical Engineers*, vol. 113, no. 7, 1966, pp. 1151–1158.

[2] T. H. Maiman, "Stimulated optical radiation in ruby," *Nature*, vol. 187, no. 4736, pp. 493–494, 1960.

[3] R. N. Hall, G. Fenner, J. Kingsley, T. Soltys, and R. Carlson, "Coherent light emission from GaAs junctions," *Physical Review Letters*, vol. 9, no. 9, pp. 366–368, 1962.

[4] M. I. Nathan, W. P. Dumke, G. Burns, F. H. Dill Jr, and G. Lasher, "Stimulated emission of radiation from GaAs pn junctions," *Applied Physics Letters*, vol. 1, no. 3, pp. 62–64, 1962.

[5] R. J. Mears, L. Reekie, I. Jauncey, and D. N. Payne, "Low-noise Erbium-doped fibre amplifier operating at 1.54 μm," *Electronics Letters*, vol. 23, no. 19, pp. 1026–1028, 1987.

[6] E. Agrell, M. Karlsson, A. R. Chraplyvy, D. J. Richardson, P. M. Krummrich, P. Winzer, K. Roberts, J. K. Fischer, S. J. Savory, B. J. Eggleton, M. Secondini, F. R. Kschischang, A. Lord, J. Prat, I. Tomkos, J. E. Bowers, S. Srinivasan, M. Brandt-Pearce, and N. Gisin, "Roadmap of optical communications," *Journal of Optics*, vol. 18, no. 6, p. 063002, 2016.

[7] P. J. Winzer and R.-J. Essiambre, "Advanced modulation formats for high-capacity optical transport networks," *Journal of Lightwave Technology*, vol. 24, no. 12, pp. 4711–4728, 2006.

[8] L. Grüner-Nielsen, M. Wandel, P. Kristensen, C. Jørgensen, L. V. Jørgensen, B. Edvold, B. Pálsdóttir, and D. Jakobsen, "Dispersion-compensating fibers," *Journal of Lightwave Technology*, vol. 23, no. 11, pp. 3566–3579, 2005.

[9] K. O. Hill and G. Meltz, "Fiber Bragg grating technology fundamentals and overview," *Journal of Lightwave Technology*, vol. 15, no. 8, pp. 1263–1276, 1997.

[10] J.-X. Cai, H. G. Batshon, M. V. Mazurczyk, O. V. Sinkin, D. Wang, M. Paskov, W. W. Patterson, C. R. Davidson, P. C. Corbett, G. M. Wolter, T. E. Hammon, M. A. Bolshtyansky, D. G. Foursa, and A. N. Pilipetskii, "70.46 Tb/s over 7,600 km and 71.65 Tb/s over 6,970 km transmission in C+L band using coded modulation with hybrid constellation shaping and nonlinearity compensation," *Journal of Lightwave Technology*, vol. 36, no. 1, pp. 114–121, 2018.

[11] E. Agrell and M. Karlsson, "Power-efficient modulation formats in coherent transmission systems," *Journal of Lightwave Technology*, vol. 27, no. 22, pp. 5115–5126, 2009.

[12] T. A. Eriksson, M. Sjödin, P. Johannisson, P. A. Andrekson, and M. Karlsson, "Comparison of 128-SP-QAM and PM-16QAM in long-haul WDM transmission," *Optics Express*, vol. 21, no. 16, pp. 19 269–19 279, 2013.

[13] M. Terayama, S. Okamoto, K. Kasai, M. Yoshida, and M. Nakazawa, "4096 QAM (72 Gbit/s) single-carrier coherent optical transmission with a potential SE of 15.8 bit/s/Hz in all-Raman amplified 160 km fiber link," in *Optical Fiber Communication Conference (OFC)*, 2018, p. Th1F.2.

[14] A. Ghazisaeidi, I. F. de Jauregui Ruiz, R. Rios-Müller, L. Schmalen, P. Tran, P. Brindel, A. C. Meseguer, Q. Hu, F. Buchali, G. Charlet, and J. Renaudier, "Advanced C+L-band transoceanic transmission systems based on probabilistically shaped PDM-64QAM," *Journal of Lightwave Technology*, vol. 35, no. 7, pp. 1291–1299, 2017.

[15] F. Chang, K. Onohara, and T. Mizuochi, "Forward error correction for 100 G transport networks," *IEEE Communications Magazine*, vol. 48, no. 3, pp. S48–S55, 2010.

[16] S. J. Savory, "Digital coherent optical receivers: algorithms and subsystems," *IEEE Journal of Selected Topics in Quantum Electronics*, vol. 16, no. 5, pp. 1164–1179, 2010.

[17] S. J. Savory, G. Gavioli, R. I. Killey, and P. Bayvel, "Electronic compensation of chromatic dispersion using a digital coherent receiver," *Optics Express*, vol. 15, no. 5, pp. 2120–2126, 2007.

[18] C. Shannon, "A mathematical theory of communication," *Bell System Technical Journal*, vol. 27, no. 3, pp. 379–423, 1948.

[19] R. Olshansky, "Noise figure for Erbium-doped optical fibre amplifiers," *Electronics Letters*, vol. 24, no. 22, pp. 1363–1365, 1988.

[20] R. Stolen and A. Ashkin, "Optical Kerr effect in glass waveguide," *Applied Physics Letters*, vol. 22, no. 6, pp. 294–296, 1973.

[21] R.-J. Essiambre, G. Kramer, P. J. Winzer, G. J. Foschini, and B. Goebel, "Capacity limits of optical fiber networks," *Journal of Lightwave Technology*, vol. 28, no. 4, pp. 662–701, 2010.

[22] A. D. Ellis, J. Zhao, and D. Cotter, "Approaching the non-linear shannon limit," *Journal of Lightwave Technology*, vol. 28, no. 4, pp. 423–433, 2010.

[23] A. Hasegawa, "An historical review of application of optical solitons for high speed communications," *Chaos*, vol. 10, no. 3, 2000.

[24] B. Hermansson and D. Yevick, "Numerical investigation of soliton interaction," *Electronics Letters*, vol. 19, no. 15, pp. 570–571, 1983.

[25] J. P. Gordon and H. A. Haus, "Random walk of coherently amplified solitons in optical fiber transmission," *Optics Letters*, vol. 11, no. 10, pp. 665–667, 1986.

[26] R. A. Fisher, B. R. Suydam, and D. Yevick, "Optical phase conjugation for time-domain undoing of dispersive self-phase-modulation effects," *Optics Letters*, vol. 8, no. 12, pp. 611–613, 1983.

[27] W. Pieper, C. Kurtzke, R. Schnabel, D. Breuer, R. Ludwig, K. Petermann, and H. Weber, "Nonlinearity-insensitive standard-fibre transmission based on optical-phase conjugation in a semiconductor-laser amplifier," *Electronics Letters*, vol. 30, no. 9, pp. 724–726, 1994.

[28] H. Hu, R. M. Jopson, A. Gnauck, M. Dinu, S. Chandrasekhar, X. Liu, C. Xie, M. Montoliu, S. Randel, and C. McKinstrie, "Fiber nonlinearity compensation of an 8-channel WDM PDM-QPSK signal using multiple phase conjugations," in *Optical Fiber Communication Conference (OFC)*, 2014, p. M3C.2.

[29] A. D. Ellis, M. E. McCarthy, M. A. Z. Al-Khateeb, and S. Sygletos, "Capacity limits of systems employing multiple optical phase conjugators," *Optics Express*, vol. 23, no. 16, pp. 20 381–20 393, 2015.

[30] K. Solis-Trapala, T. Inoue, and S. Namiki, "Signal power asymmetry tolerance of an optical phase conjugation-based nonlinear compensation system," in *European Conference on Optical Communications (ECOC)*, 2014, p. We.2.5.4.

[31] K. Solis-Trapala, M. Pelusi, H. N. Tan, T. Inoue, and S. Namiki, "Transmission optimized impairment mitigation by 12 stage phase conjugation of WDM 24×48 Gb/s DP-QPSK signals," in *Optical Fiber Communication Conference (OFC)*, 2015, p. Th3C.2.

[32] R. Essiambre and P. Winzer, "Fibre nonlinearities in electronically predistorted transmission," in *European Conference on Optical Communications (ECOC)*, vol. 2, 2005, pp. 191–192.

[33] E. Ip and J. M. Kahn, "Compensation of dispersion and nonlinear impairments using digital backpropagation," *Journal of Lightwave Technology*, vol. 26, no. 20, pp. 3416–3425, 2008.

[34] D. Rafique, M. Mussolin, M. Forzati, J. Mårtensson, M. N. Chugtai, and A. D. Ellis, "Compensation of intra-channel nonlinear fibre impairments using simplified digital back-propagation algorithm," *Optics Express*, vol. 19, no. 10, pp. 9453–9460, 2011.

[35] E. Temprana, E. Myslivets, L. Liu, V. Ataie, A. Wiberg, B. P. P. Kuo, N. Alic, and S. Radic, "Two-fold transmission reach enhancement enabled by transmitter-side digital backpropagation and optical frequency comb-derived information carriers." *Optics Express*, vol. 23, no. 16, pp. 20 774–20 783, 2015.

[36] E. Temprana, E. Myslivets, V. Ataie, B. P. P. Kuo, N. Alic, V. Vusirikala, V. Dangui, and S. Radic, "Demonstration of coherent transmission reach tripling by frequency-referenced nonlinearity pre-compensation in edfa-only smf link," in *European Conference on Optical Communications (ECOC)*, 2016, p. Tu.3.B.4.

[37] R. Maher, T. Xu, L. Galdino, M. Sato, A. Alvarado, K. Shi, S. J. Savory, B. C. Thomsen, R. I. Killey, and P. Bayvel, "Spectrally shaped DP-16QAM super-channel transmission with multi-channel digital backpropagation," *Nature Scientific Reports*, vol. 5, 2015.

[38] C. B. Czegledi, G. Liga, D. Lavery, M. Karlsson, E. Agrell, S. J. Savory, and P. Bayvel, "Digital backpropagation accounting for polarization-mode dispersion," *Optics Express*, vol. 25, no. 3, pp. 1903–1915, 2017.

[39] M. I. Yousefi and F. R. Kschischang, "Information transmission using the nonlinear Fourier transform, part I: Mathematical tools," *IEEE Trans. Inf. Theory*, vol. 60, no. 7, pp. 4312–4328, 2014.

[40] ——, "Information transmission using the nonlinear Fourier transform, part II: Numerical methods," *IEEE Transactions on Information Theory*, vol. 60, no. 7, pp. 4329–4345, 2014.

[41] ——, "Information transmission using the nonlinear Fourier Transform, part III: Spectrum modulation," *IEEE Transactions on Information Theory*, vol. 60, no. 7, pp. 4346–4369, 2014.

[42] S. K. Turitsyn, J. E. Prilepsky, S. T. Le, S. Wahls, L. L. Frumin, M. Kamalian, and S. A. Derevyanko, "Nonlinear Fourier transform for optical data processing and transmission: Advances and perspectives," *Optica*, vol. 4, no. 3, pp. 307–322, 2017.

[43] X. Liu, A. R. Chraplyvy, P. J. Winzer, R. W. Tkach, and S. Chandrasekhar, "Phase-conjugated twin waves for communication beyond the Kerr nonlinearity limit," *Nature Photonics*, vol. 7, no. 7, pp. 560–568, 2013.

[44] X. Liu, S. Chandrasekhar, P. J. Winzer, R. W. Tkach, and A. R. Chraplyvy, "Fiber-nonlinearity-tolerant superchannel transmission via nonlinear noise squeezing and generalized phase-conjugated twin waves," *Journal of Lightwave Technology*, vol. 32, no. 4, pp. 766–775, 2014.

[45] Y. Yu and J. Zhao, "Modified phase-conjugate twin wave schemes for fiber nonlinearity mitigation," *Optics Express*, vol. 23, no. 23, pp. 30 399–30 413, 2015.

[46] S. T. Le, M. E. McCarthy, N. M. Suibhne, M. A. Z. Al-Khateeb, E. Giacoumidis, N. Doran, A. D. Ellis, and S. K. Turitsyn, "Demonstration of phase-conjugated subcarrier coding for fiber nonlinearity compensation in CO-OFDM transmission," *Journal of Lightwave Technology*, vol. 33, no. 11, pp. 2206–2212, 2015.

[47] Y. Tian, Y.-K. Huang, S. Zhang, P. R. Prucnal, and T. Wang, "Demonstration of digital phase-sensitive boosting to extend signal reach for long-haul WDM systems using optical phase-conjugated copy," *Optics Express*, vol. 21, no. 4, pp. 5099–5106, 2013.

[48] S. L. I. Olsson, B. Corcoran, C. Lundström, M. Sjödin, M. Karlsson, and P. A. Andrekson, "Phase-sensitive amplified optical link operating in the nonlinear transmission regime," in *European Conference on Optical Communications (ECOC)*, 2012, p. Th.2.F.1.

[49] Z. Tong, C. Lundström, P. A. Andrekson, C. J. McKinstrie, M. Karlsson, D. J. Blessing, E. Tipsuwannakul, B. J. Puttnam, H. Toda, and L. Grüner-Nielsen, "Towards ultrasensitive optical links enabled by low-noise phase-sensitive amplifiers," *Nature Photonics*, vol. 5, no. 7, pp. 430–436, 2011.

[50] B. Foo, B. Corcoran, and A. J. Lowery, "Distributed nonlinear compensation using optoelectronic circuits," *Journal of Lightwave Technology*, vol. 36, no. 6, pp. 1326–1339, 2018.

[51] "Infinera Infinite Capacity Engine White Paper," https://www.infinera.com/wp-content/uploads/2016/03/Infinera-BR_Infinite-Capacity-Engine.pdf, accessed: 2018-04-05.

[52] "Corning SMF28 ULL optical fiber data sheet," https://www.corning.com/media/worldwide/coc/documents/Fiber/SMF-28%20ULL.pdf, accessed: 2018-03-29.

[53] J. Kerr, "XL. A new relation between electricity and light: Dielectrified media birefringent," *The London, Edinburgh, and Dublin Philosophical Magazine and Journal of Science*, vol. 50, no. 332, pp. 337–348, 1875.

[54] ——, "LIV. A new relation between electricity and light: Dielectrified media birefringent (second paper)," *The London, Edinburgh, and Dublin Philosophical Magazine and Journal of Science*, vol. 50, no. 333, pp. 446–458, 1875.

[55] D. Wang and C. R. Menyuk, "Polarization evolution due to the Kerr nonlinearity and chromatic dispersion," *Journal of Lightwave Technology*, vol. 17, no. 12, pp. 2520–2529, 1999.

[56] G. P. Agrawal, *Fiber-optic communication systems*, 4th ed. John Wiley & Sons, 2010.

[57] C. M. Caves, "Quantum limits on noise in linear amplifiers," *Physical Review D*, vol. 26, no. 8, pp. 1817–1839, 1982.

[58] Y. Yamamoto and H. A. Haus, "Preparation, measurement and information capacity of optical quantum states," *Reviews of Modern Physics*, vol. 58, pp. 1001–1020, 1986.

[59] Z. Tong and S. Radic, "Low-noise optical amplification and signal processing in parametric devices," *Advances in Optics and Photonics*, vol. 5, no. 3, pp. 318–384, 2013.

[60] C. V. Raman, "A new radiation," *Indian Journal of Physics*, vol. 2, pp. 387–398, 1928.

[61] R. H. Stolen, E. Ippen, and A. Tynes, "Raman oscillation in glass optical waveguide," *Applied Physics Letters*, vol. 20, no. 2, pp. 62–64, 1972.

[62] G. P. Agrawal, *Nonlinear fiber optics*, 4th ed. Elsevier academic press, 2007.

[63] S. L. Olsson, J. Cho, S. Chandrasekhar, X. Chen, P. J. Winzer, and S. Makovejs, "Probabilistically shaped PDM 4096-QAM transmission over up to 200 km of fiber using standard intradyne detection," *Optics Express*, vol. 26, no. 4, pp. 4522–4530, 2018.

[64] C. Headley and G. P. Agrawal, *Raman amplification in fiber optical communication systems*. Elsevier academic press, 2005.

[65] H. T. Friis, "Noise figures of radio receivers," *Proceedings of the IRE*, vol. 32, no. 7, pp. 419–422, 1944.

[66] K. Rottwitt, A. Stentz, T. Nielsen, P. Hansen, K. Feder, and K. Walker, "Transparent 80 km bi-directionally pumped distributed Raman amplifier with second order pumping," in *European Conference on Optical Communications (ECOC)*, vol. 2, 1999, pp. 144–145.

[67] J.-C. Bouteiller, K. Brar, and C. Headley, "Quasi-constant signal power transmission," in *European Conference on Optical Communications (ECOC)*, 2002, p. S3.04.

[68] J. D. Ania-Castañón, "Quasi-lossless transmission using second-order Raman amplification and fibre Bragg gratings," *Optics Express*, vol. 12, no. 19, pp. 4372–4377, 2004.

[69] M. Tan, P. Rosa, S. T. Le, I. D. Phillips, and P. Harper, "Evaluation of 100G DP-QPSK long-haul transmission performance using second order co-pumped Raman laser based amplification," *Optics Express*, vol. 23, no. 17, pp. 22 181–22 189, 2015.

[70] L. A. Coldren, S. W. Corzine, and M. L. Mashanovitch, *Diode lasers and photonic integrated circuits*. John Wiley & Sons, 2012, vol. 218.

[71] C. R. S. Fludger, V. Handerek, and R. J. Mears, "Pump to signal RIN transfer in Raman fiber amplifiers," *Journal of Lightwave Technology*, vol. 19, no. 8, pp. 1140–1148, 2001.

[72] J. Cheng, M. Tang, A. P. T. Lau, C. Lu, L. Wang, Z. Dong, S. M. Bilal, S. Fu, P. P. Shum, and D. Liu, "Pump RIN-induced impairments in unrepeatered transmission systems using distributed Raman amplifier," *Optics Express*, vol. 23, no. 9, pp. 11 838–11 854, 2015.

[73] P. B. Hansen, L. Eskildsen, J. Stentz, T. A. Strasser, J. Judkins, J. J. DeMarco, R. Pedrazzani, and D. J. DiGiovanni, "Rayleigh scattering limitations in distributed Raman pre-amplifiers," *IEEE Photonics Technology Letters*, vol. 10, no. 1, pp. 159–161, 1998.

[74] R. J. Essiambre, P. Winzer, J. Bromage, and C. H. Kim, "Design of bidirectionally pumped fiber amplifiers generating double Rayleigh backscattering," *IEEE Photonics Technology Letters*, vol. 14, no. 7, pp. 914–916, 2002.

[75] S. Faralli and F. D. Pasquale, "Impact of double Rayleigh scattering noise in distributed higher order Raman pumping schemes," *IEEE Photonics Technology Letters*, vol. 15, no. 6, pp. 804–806, 2003.

[76] T. R. Taha and M. I. Ablowitz, "Analytical and numerical aspects of certain nonlinear evolution equations. II. Numerical, nonlinear schrödinger equation," *Journal of Computational Physics*, vol. 55, no. 2, pp. 203 – 230, 1984.

[77] O. V. Sinkin, R. Holzlöhner, J. Zweck, and C. R. Menyuk, "Optimization of the split-step fourier method in modeling optical-fiber communications systems," *Journal of Lightwave Technology*, vol. 21, no. 1, pp. 61–68, 2003.

[78] Y. Gao, J. C. Cartledge, A. S. Karar, S. S.-H. Yam, M. O'Sullivan, C. Laperle, A. Borowiec, and K. Roberts, "Reducing the complexity of perturbation based nonlinearity pre-compensation using symmetric EDC and pulse shaping," *Optics Express*, vol. 22, no. 2, pp. 1209–1219, 2014.

[79] F. P. Guiomar, J. D. Reis, A. Carena, G. Bosco, A. L. Teixeira, and A. N. Pinto, "Experimental demonstration of a frequency-domain Volterra series nonlinear equalizer in polarization-multiplexed transmission," *Optics Express*, vol. 21, no. 1, pp. 276–288, 2013.

[80] H.-M. Chin, M. Forzati, and J. Mårtensson, "Volterra based nonlinear compensation on 224 Gb/s PolMux-16QAM optical fibre link," in *National Fiber Optic Engineers Conference (NFOEC)*, 2012, p. JW2A.61.

[81] N. V. Irukulapati, H. Wymeersch, P. Johannisson, and E. Agrell, "Stochastic digital backpropagation," *IEEE Transactions on Communications*, vol. 62, no. 11, pp. 3956–3968, 2014.

[82] A. Mecozzi, C. B. Clausen, and M. Shtaif, "Analysis of intrachannel nonlinear effects in highly dispersed optical pulse transmission," *IEEE Photonics Technology Letters*, vol. 12, no. 4, pp. 392–394, 2000.

[83] P. Poggiolini, "The GN model of non-linear propagation in uncompensated coherent optical systems," *Journal of Lightwave Technology*, vol. 30, no. 24, pp. 3857–3879, 2012.

[84] V. Curri, A. Carena, P. Poggiolini, G. Bosco, and F. Forghieri, "Extension and validation of the GN model for non-linear interference to uncompensated links using Raman amplification," *Optics Express*, vol. 21, no. 3, pp. 3308–3317, 2013.

[85] W. S. Pelouch, "Raman amplification: An enabling technology for long-haul coherent transmission systems," *Journal of Lightwave Technology*, vol. 34, no. 1, pp. 6–19, 2016.

[86] X. Wei, "Power-weighted dispersion distribution function for characterizing nonlinear properties of long-haul optical transmission links," *Optics Letters*, vol. 31, no. 17, pp. 2544–2546, 2006.

[87] A. Yariv, D. Fekete, and D. M. Pepper, "Compensation for channel dispersion by nonlinear optical phase conjugation," *Optics Letters*, vol. 4, no. 2, pp. 52–54, 1979.

[88] R. M. Jopson and R. E. Tench, "Polarisation-independent phase conjugation of lightwave signals," *Electronics Letters*, vol. 29, no. 25, pp. 2216–2217, 1993.

[89] P. O. Hedekvist, M. Karlsson, and P. A. Andrekson, "Polarization dependence and efficiency in a fiber four-wave mixing phase conjugator with orthogonal pump waves," *IEEE Photonics Technology Letters*, vol. 8, no. 6, pp. 776–778, 1996.

[90] S. Watanabe, T. Naito, and T. Chikama, "Compensation of chromatic dispersion in a single-mode fiber by optical phase conjugation," *IEEE Photonics Technology Letters*, vol. 5, no. 1, pp. 92–95, 1993.

[91] S. Watanabe and M. Shirasaki, "Exact compensation for both chromatic dispersion and Kerr effect in a transmission fiber using optical phase conjugation," *Journal of Lightwave Technology*, vol. 14, no. 3, pp. 243–248, 1996.

[92] C. Lorattanasane and K. Kikuchi, "Design theory of long-distance optical transmission systems using midway optical phase conjugation," *Journal of Lightwave Technology*, vol. 15, no. 6, pp. 948–955, 1997.

[93] G. Woods, P. Papaparaskeva, M. Shtaif, I. Brener, and D. Pitt, "Reduction of cross-phase modulation-induced impairments in long-haul WDM telecommunication systems via spectral inversion," *IEEE Photonics Technology Letters*, vol. 16, no. 2, pp. 677–679, 2004.

[94] S. Jansen, D. Van Den Borne, P. Krummrich, S. Spalter, G. Khoe, and H. De Waardt, "Long-haul DWDM transmission systems employing optical phase conjugation," *IEEE Journal of Selected Topics in Quantum Electronics*, vol. 12, no. 4, pp. 505–520, 2006.

[95] P. Kaewplung and K. Kikuchi, "Simultaneous cancellation of fiber loss, dispersion, and Kerr effect in ultralong-haul optical fiber transmission by midway optical phase conjugation incorporated with distributed Raman amplification," *Journal of Lightwave Technology*, vol. 25, no. 10, pp. 3035–3050, 2007.

[96] W. Kuperman, W. S. Hodgkiss, H. C. Song, T. Akal, C. Ferla, and D. R. Jackson, "Phase conjugation in the ocean: Experimental demonstration of an acoustic time-reversal mirror," *The Journal of the Acoustical Society of America*, vol. 103, no. 1, pp. 25–40, 1998.

[97] G. Lerosey, J. De Rosny, A. Tourin, A. Derode, G. Montaldo, and M. Fink, "Time reversal of electromagnetic waves," *Physical Review Letters*, vol. 92, no. 19, p. 193904, 2004.

[98] G. He, "Optical phase conjugation: principles, techniques, and applications," *Progress in Quantum Electronics*, vol. 26, no. 3, pp. 131–191, 2002.

[99] A. Yariv and D. M. Pepper, "Amplified reflection, phase conjugation, and oscillation in degenerate four-wave mixing," *Optics Letters*, vol. 1, no. 1, pp. 16–18, 1977.

[100] A. Heuer and R. Menzel, "Phase-conjugating stimulated Brillouin scattering mirror for low powers and reflectivities above 90% in an internally tapered optical fiber," *Optics Letters*, vol. 23, no. 11, pp. 834–836, 1998.

[101] B.-E. Olsson, C. Larsson, J. Mårtensson, and A. Alping, "Experimental demonstration of electro-optical mid-span spectrum inversion for mitigation of non-linear fiber effects," in *European Conference on Optical Communications (ECOC)*, 2012, p. Th.1.D.4.

[102] M. C. Tatham, G. Sherlock, and L. D. Westbrook, "Compensation fibre chromatic dispersion by optical phase conjugation in a semiconductor laser amplifier," *Electronics Letters*, vol. 29, no. 21, pp. 1851–1852, 1993.

[103] S. Radic and C. J. McKinstrie, "Optical amplification and signal processing in highly nonlinear optical fiber," *IEICE Transactions on Electronics*, vol. 88, no. 5, pp. 859–869, 2005.

[104] R. Tang, J. Lasri, P. S. Devgan, V. Grigoryan, P. Kumar, and M. Vasilyev, "Gain characteristics of a frequency nondegenerate phase-sensitive fiber-optic parametric amplifier with phase self-stabilized input," *Optics Express*, vol. 13, no. 26, pp. 10 483–10 493, 2005.

[105] X. Liu, H. Hu, S. Chandrasekhar, R. M. Jopson, A. H. Gnauck, M. Dinu, C. Xie, and P. J. Winzer, "Generation of 1.024-Tb/s Nyquist-WDM phase-conjugated twin vector waves by a polarization-insensitive optical parametric amplifier for fiber-nonlinearity-tolerant transmission," *Optics Express*, vol. 22, no. 6, pp. 6478–6485, 2014.

[106] A. Lorences-Riesgo, F. Chiarello, C. Lundström, M. Karlsson, and P. A. Andrekson, "Experimental analysis of degenerate vector phase-sensitive amplification," *Optics Express*, vol. 22, no. 18, pp. 21 889–21 902, 2014.

[107] C. McKinstrie and S. Radic, "Phase-sensitive amplification in a fiber," *Optics Express*, vol. 12, no. 20, pp. 4973–4979, 2004.

[108] R. A. Fisher, *Optical phase conjugation*. Academic Press, 2012.

[109] M. Mazur, A. Lorences-Riesgo, J. Schröder, P. A. Andrekson, and M. Karlsson, "High spectral efficiency PM-128QAM comb-based superchannel transmission enabled by a single shared optical pilot tone," *Journal of Lightwave Technology*, vol. 36, no. 6, pp. 1318–1325, 2018.

[110] A. Lorences-Riesgo, P. A. Andrekson, and M. Karlsson, "Polarization-independent phase-sensitive amplification," *Journal of Lightwave Technology*, vol. 34, no. 13, pp. 3171–3180, 2016.

[111] A. Fülöp, M. Mazur, A. Lorences-Riesgo, T. A. Eriksson, P.-H. Wang, Y. Xuan, D. E. Leaird, M. Qi, P. A. Andrekson, A. M. Weiner, and V. Torres-Company, "Long-haul coherent communications using microresonator-based frequency combs," *Optics Express*, vol. 25, no. 22, pp. 26 678–26 688, 2017.

[112] A. Klekamp and F. Buchali, "Coherent intradyne opto-electro-optic spectral inverter and its application for SPM mitigation and wavelength conversion," in *European Conference on Optical Communications (ECOC)*, 2013, p. We.3.C.5.

[113] J. Hansryd, P. A. Andrekson, M. Westlund, J. Li, and P. O. Hedekvist, "Fiber-based optical parametric amplifiers and their applications," *IEEE Journal of Selected Topics in Quantum Electronics*, vol. 8, no. 3, pp. 506–520, May 2002.

[114] T. Umeki, O. Tadanaga, A. Takada, and M. Asobe, "Phase sensitive degenerate parametric amplification using directly-bonded PPLN ridge waveguides," *Optics Express*, vol. 19, no. 7, pp. 6326–6332, 2011.

[115] Y. Zhang, C. Husko, J. Schröder, S. Lefrancois, I. H. Rey, T. F. Krauss, and B. J. Eggleton, "Phase-sensitive amplification in silicon photonic crystal waveguides," *Optics Letters*, vol. 39, no. 2, pp. 363–366, 2014.

[116] H. Sun, K.-Y. Wang, and A. C. Foster, "Pump-degenerate phase-sensitive amplification in amorphous silicon waveguides," *Optics Letters*, vol. 42, no. 18, pp. 3590–3593, 2017.

[117] S. L. I. Olsson, M. Karlsson, and P. A. Andrekson, "Nonlinear phase noise mitigation in phase-sensitive amplified transmission systems," *Optics Express*, vol. 23, no. 9, pp. 11 724–11 740, 2015.

[118] R. Slavík, F. Parmigiani, J. Kakande, C. Lundström, M. Sjödin, P. A. Andrekson, R. Weerasuriya, S. Sygletos, A. D. Ellis, L. Grüner-Nielsen, D. Jakobsen, S. Herstrøm, R. Phelan, J. O´Gorman, A. Bogris, D. Syvridis, S. Dasgupta, P. Petropoulos, and D. J. Richardson, "All-optical phase and amplitude regenerator for next-generation telecommunications systems," *Nature Photonics*, vol. 4, no. 10, pp. 690–695, 2010.

[119] T. Umeki, M. Asobe, H. Takara, Y. Miyamoto, and H. Takenouchi, "Multi-span transmission using phase and amplitude regeneration in PPLN-based PSA," *Optics Express*, vol. 21, no. 15, pp. 18 170–18 177, 2013.

[120] W. Xie, I. Fsaifes, and F. Bretenaker, "Optimization of a degenerate dual-pump phase-sensitive optical parametric amplifier for all-optical regenerative functionality," *Optics Express*, vol. 25, no. 11, pp. 12 552–12 565, 2017.

[121] J. N. Kutz, C. V. Hile, W. L. Kath, R.-D. Li, and P. Kumar, "Pulse propagation in nonlinear optical fiber lines that employ phase-sensitive parametric amplifiers," *Journal of the Optical Society of America B*, vol. 11, no. 10, pp. 2112–2123, 1994.

[122] M. Vasilyev, "Distributed phase-sensitive amplification," *Optics Express*, vol. 13, no. 19, pp. 7563–7571, 2005.

[123] P. Minzioni, "Nonlinearity compensation in a fiber-optic link by optical phase conjugation," *Fiber and Integrated Optics*, vol. 28, no. 3, pp. 179–209, 2009.

[124] A. D. Ellis, M. Tan, M. A. Iqbal, M. A. Z. Al-Khateeb, V. Gordienko, G. S. Mondaca, S. Fabbri, M. F. C. Stephens, M. E. McCarthy, A. Perentos, I. D. Phillips, D. Lavery, G. Liga, R. Maher, P. Harper, N. Doran, S. K. Turitsyn, S. Sygletos, and P. Bayvel, "4 Tb/s transmission reach enhancement using 10 × 400 Gb/s super-channels and polarization insensitive dual band optical phase conjugation," *Journal of Lightwave Technology*, vol. 34, no. 8, pp. 1717–1723, 2016.

[125] T. Kobayashi, T. Umeki, R. Kasahara, H. Yamazaki, M. Nagatani, H. Wakita, H. Takenouchi, and Y. Miyamoto, "96-Gbaud PDM-8QAM single channel transmission over 9,600 km by nonlinear tolerance enhancement using PPLN-based optical phase conjugation," in *Optical Fiber Communication Conference (OFC)*, 2018, p. Th3E.4.

[126] Y. Sun, A. Lorences-Riesgo, F. Parmigiani, K. R. Bottrill, S. Yoshima, G. D. Hesketh, M. Karlsson, P. A. Andrekson, D. J. Richardson, and P. Petropoulos, "Optical nonlinearity mitigation of 6 × 10 GBd polarization-division multiplexing 16 QAM signals in a field-installed transmission link," in *Optical Fiber Communication Conference (OFC)*, 2017, p. Th3J.2.

[127] P. Rosa, S. T. Le, G. Rizzelli, M. Tan, and J. D. Ania-Castañón, "Signal power asymmetry optimisation for optical phase conjugation using Raman amplification," *Optics Express*, vol. 23, no. 25, pp. 31 772–31 778, 2015.

[128] I. Phillips, M. Tan, M. Stephens, M. McCarthy, E. Giacoumidis, S. Sygletos, P. Rosa, S. Fabbri, S. Le, T. Kanesan, S. Turitsyn, N. Doran, P. Harper, and A. Ellis, "Exceeding the nonlinear-Shannon limit using Raman laser based amplification and optical phase conjugation," in *Optical Fiber Communication Conference (OFC)*, 2014, p. M3C.1.

[129] M. D. Pelusi, "WDM signal all-optical precompensation of Kerr nonlinearity in dispersion-managed fibers," *IEEE Photonics Technology Letters*, vol. 25, no. 1, pp. 71–74, 2013.

[130] S. Yoshima, Y. Sun, Z. Liu, K. R. H. Bottrill, F. Parmigiani, D. J. Richardson, and P. Petropoulos, "Mitigation of nonlinear effects on WDM QAM signals enabled by optical phase conjugation with efficient bandwidth utilization," *Journal of Lightwave Technology*, vol. 35, no. 4, pp. 971–978, 2017.

[131] M. E. McCarthy, M. A. Z. Al Kahteeb, F. M. Ferreira, and A. D. Ellis, "PMD tolerant nonlinear compensation using in-line phase conjugation," *Optics Express*, vol. 24, no. 4, pp. 3385–3392, 2016.

[132] X. Liu, S. Chandrasekhar, A. H. Gnauck, P. J. Winzer, S. Randel, S. Corteselli, A. R. Chraplyvy, R. W. Tkach, B. Zhu, T. F. Taunay, and M. Fishteyn, "Digital coherent superposition for performance improvement of spatially multiplexed coherent optical OFDM superchannels," *Optics Express*, vol. 20, no. 26, pp. B595–B600, 2012.

[133] K. Kuchi, R. Vinod, M. K. Dileep, M. S. Padmanabhan, B. Dhivagar, J. K. Milleth, B. Ramamurthi, and K. Giridhar, "Interference mitigation using conjugate data repetition," in *IEEE International Conference on Communications (ICC)*, 2009.

[134] W. H. McMaster, "Matrix representation of polarization," *Reviews of Modern Physics*, vol. 33, no. 1, pp. 8–28, 1961.

[135] P. Johannisson, M. Sjödin, M. Karlsson, H. Wymeersch, E. Agrell, and P. A. Andrekson, "Modified constant modulus algorithm for polarization-switched QPSK," *Optics Express*, vol. 19, no. 8, pp. 7734–7741, 2011.

[136] Z. Zheng, X. Lv, F. Zhang, D. Wang, E. Sun, Y. Zhu, K. Zou, and Z. Chen, "Fiber nonlinearity mitigation in 32-Gbaud 16QAM Nyquist-WDM systems," *Journal of Lightwave Technology*, vol. 34, no. 9, pp. 2182–2187, 2016.

[137] M. Secondini and E. Forestieri, "On XPM mitigation in WDM fiber-optic systems," *IEEE Photonics Technology Letters*, vol. 26, no. 22, pp. 2252–2255, 2014.

[138] K. O. Hill, F. Bilodeau, B. Malo, T. Kitagawa, S. Thériault, D. C. Johnson, J. Albert, and K. Takiguchi, "Chirped in-fiber Bragg gratings for compensation of optical-fiber dispersion," *Optics Letters*, vol. 19, no. 17, pp. 1314–1316, 1994.

[139] X. Liu, S. Chandrasekhar, P. J. Winzer, B. Maheux-L, G. Brochu, and F. Trepanier, "Efficient fiber nonlinearity mitigation in 50-GHz-DWDM transmission of 256-Gb/s PDM-16QAM signals by folded digital-back-propagation and channelized FBG-DCMs," in *Optical Fiber Communication Conference (OFC)*, 2014, p. Tu3A.8.

[140] B. J. Eggleton, J. A. Rogers, P. S. Westbrook, and T. A. Strasser, "Electrically tunable power efficient dispersion compensating fiber Bragg grating," *IEEE Photonics Technology Letters*, vol. 11, no. 7, pp. 854–856, 1999.

[141] B. J. Eggleton, A. Ahuja, P. S. Westbrook, J. A. Rogers, P. Kuo, T. N. Nielsen, and B. Mikkelsen, "Integrated tunable fiber gratings for dispersion management in high-bit rate systems," *Journal of Lightwave Technology*, vol. 18, no. 10, pp. 1418–1432, 2000.

[142] X. Shu, K. Sugden, P. Rhead, J. Mitchell, I. Felmeri, G. Lloyd, K. Byron, Z. Huang, I. Khrushchev, and I. Bennion, "Tunable dispersion compensator based on distributed Gires-Tournois etalons," *IEEE Photonics Technology Letters*, vol. 15, no. 8, pp. 1111–1113, 2003.

[143] M. Sumetsky, B. J. Eggleton, and C. M. de Sterke, "Theory of group delay ripple generated by chirped fiber gratings," *Optics Express*, vol. 10, no. 7, pp. 332–340, 2002.

[144] E. Tipsuwannakul, J. Li, T. A. Eriksson, L. Egnell, F. Sjöström, J. Pejnefors, P. A. Andrekson, and M. Karlsson, "Influence of fiber-Bragg grating-induced group-delay ripple in high-speed transmission systems," *Journal of Optical Communications and Networking*, vol. 4, no. 6, pp. 514–521, 2012.

[145] *Data sheet ClearSpectrum DCML - Dispersion Compensation Module*, TeraXion, 2013, accessed 2018-02-27. [Online]. Available: http://www.teraxion.com/images/stories/pdf/MKT-FTECH-CS-DCML_201306-3.0.pdf

[146] N. Litchinitser, Y. Li, M. Sumetsky, P. Westbrook, and B. Eggleton, "Tunable dispersion compensation devices: group delay ripple and system performance," in *Optical Fiber Communication Conference (OFC)*, 2003, p. TuD2.

[147] C. J. McKinstrie, J. M. Dailey, A. Agarwal, and P. Toliver, "Optical filtering enabled by cascaded parametric amplification," *Optics Express*, vol. 24, no. 13, pp. 14 242–14 259, 2016.

[148] J. M. Dailey, A. Agarwal, C. J. McKinstrie, and P. Toliver, "Optical signal filtering using phase-sensitive amplification and de-amplification," *IEEE Photonics Technology Letters*, vol. 28, no. 16, pp. 1743–1746, 2016.

[149] B. Zheng, Q. Xie, and C. Shu, "Raman-assisted phase-sensitive amplification enabled optical add-drop filter," *IEEE Photonics Technology Letters*, vol. 29, no. 23, pp. 2047–2050, 2017.

[150] B. Corcoran, S. L. I. Olsson, C. Lundström, M. Karlsson, and P. A. Andrekson, "Mitigation of nonlinear impairments on QPSK data in phase-sensitive amplified links," in *European Conference on Optical Communications (ECOC)*, 2013, p. We.3.A.1.

[151] S. L. I. Olsson, B. Corcoran, C. Lundström, T. Eriksson, M. Karlsson, and P. A. Andrekson, "Phase-sensitive amplified transmission links for improved sensitivity and nonlinearity tolerance," *Journal of Lightwave Technology*, vol. 33, no. 3, pp. 710–721, 2015.

[152] S. L. I. Olsson, M. Karlsson, and P. A. Andrekson, "Long-haul optical transmission of 16-QAM signal with in-line phase-sensitive amplifiers," in *European Conference on Optical Communications (ECOC)*, 2017, p. W.3.B.3.

[153] Z. Tong, C. Lundström, P. A. Andrekson, M. Karlsson, and A. Bogris, "Ultralow noise, broadband phase-sensitive optical amplifiers, and their applications," *IEEE Journal of Selected Topics in Quantum Electronics*, vol. 18, no. 2, pp. 1016–1032, 2012.

[154] Y. Frignac and S. Bigo, "Numerical optimization of residual dispersion in dispersion-managed systems at 40 Gbit/s," in *Optical Fiber Communication Conference (OFC)*, 2000, p. TuD3.

[155] V. E. Perlin and H. G. Winful, "On distributed Raman amplification for ultrabroad-band long-haul WDM systems," *Journal of Lightwave Technology*, vol. 20, no. 3, p. 409, 2002.

[156] Y. Okamura, M. Abe, K. Kondo, Y. Ohmichi, T. Kazama, T. Umeki, M. Koga, and A. Takada, "Optical pump phase locking to a carrier wave extracted from phase-conjugated twin waves for phase-sensitive optical amplifier repeaters," *Optics Express*, vol. 24, no. 23, pp. 26 300–26 306, 2016.

[157] T. Umeki, T. Kazama, A. Sano, K. Shibahara, K. Suzuki, M. Abe, H. Takenouchi, and Y. Miyamoto, "Simultaneous nonlinearity mitigation in 92 × 180-Gbit/s PDM-16QAM transmission over 3840 km using PPLN-based guard-band-less optical phase conjugation," *Optics Express*, vol. 24, no. 15, pp. 16 945–16 951, 2016.

[158] R. Malik, A. Kumpera, M. Karlsson, and P. A. Andrekson, "Demonstration of ultra wideband phase-sensitive fiber optical parametric amplifier," *IEEE Photonics Technology Letters*, vol. 28, no. 2, pp. 175–177, 2016.

[159] A. D. Ellis, M. E. McCarthy, M. A. Z. A. Khateeb, M. Sorokina, and N. J. Doran, "Performance limits in optical communications due to fiber nonlinearity," *Advances in Optics and Photonics*, vol. 9, no. 3, pp. 429–503, 2017.

[160] A. A. I. Ali, C. S. Costa, M. A. Z. Al-Khateeb, F. M. Ferreira, and A. D. Ellis, "Four-wave mixing in optical phase conjugation system with pre-dispersion," in *Opto-Electronics and Communications Conference (OECC) and Photonics Global Conference (PGC)*, 2017, pp. P3–038.

[161] P. Minzioni, F. Alberti, and A. Schiffini, "Optimized link design for nonlinearity cancellation by optical phase conjugation," *IEEE Photonics Technology Letters*, vol. 16, no. 3, pp. 813–815, 2004.

[162] I. Sackey, T. Richter, M. Nölle, M. Jazayerifar, K. Petermann, J. K. Fischer, and C. Schubert, "Qualitative comparison of Kerr nonlinearity mitigation schemes in a dispersion-managed link for 4 × 28-GBd 16-QAM signals," *Journal of Lightwave Technology*, vol. 33, no. 23, pp. 4815–4825, 2015.

[163] R. G. Gallager, *Information theory and reliable communication*. John Wiley & Sons, 1968.

[164] A. Alvarado and E. Agrell, "Four-dimensional coded modulation with bit-wise decoders for future optical communications," *Journal of Lightwave Technology*, vol. 33, no. 10, pp. 1993–2003, 2015.

[165] L. Zetterberg and H. Brändström, "Codes for combined phase and amplitude modulated signals in a four-dimensional space," *IEEE Transactions on Communications*, vol. 25, no. 9, pp. 943–950, 1977.

[166] T. A. Eriksson, T. Fehenberger, P. A. Andrekson, M. Karlsson, N. Hanik, and E. Agrell, "Impact of 4D channel distribution on the achievable rates in coherent optical communication experiments," *Journal of Lightwave Technology*, vol. 34, no. 9, pp. 2256–2266, 2016.

[167] T. A. Eriksson, A. Lorences-Riesgo, P. Johannisson, T. Fehenberger, P. A. Andrekson, and M. Karlsson, "Achievable rates comparison for phase-conjugated twin-waves and PM-QPSK," in *Opto-Electronics and Communications Conference (OECC) and International Conference on Photonics in Switching (PS)*, 2016, pp. TuB3–3.

[168] M. A. Z. Al-Khateeb, M. A. Iqbal, M. Tan, A. Ali, M. McCarthy, P. Harper, and A. D. Ellis, "Analysis of the nonlinear Kerr effects in optical transmission systems that deploy optical phase conjugation," *Optics Express*, vol. 26, no. 3, pp. 3145–3160, 2018.

[169] S. Olsson, "Optical transmission systems based on phase-sensitive amplifiers," Ph.D. dissertation, 2015.

[170] C. J. McKinstrie, N. Alic, Z. Tong, and M. Karlsson, "Higher-capacity communication links based on two-mode phase-sensitive amplifiers," *Optics Express*, vol. 19, no. 13, pp. 11 977–11 991, 2011.

[171] P. M. Krummrich and M. Finkenbusch, "Selection guidelines for lumped optical amplifiers – conventional phase insensitive versus phase sensitive

parametric amplification," *Journal of Optics*, vol. 45, no. 3, pp. 269–274, 2016.

[172] J. Kim, H. Schnatz, D. S. Wu, G. Marra, D. J. Richardson, and R. Slavík, "Optical injection locking-based amplification in phase-coherent transfer of optical frequencies," *Optics Letters*, vol. 40, no. 18, pp. 4198–4201, 2015.

[173] R. Kakarla, K. Vijayan, J. Schröder, and P. A. Andrekson, "Phase noise characteristics of injection-locked lasers operated at low injection powers," in *Optical Fiber Communication Conference (OFC)*, 2018, p. M4G.2.